Conformational Analysis for Lectin-Glycan Recognition

2021. 12. 18. Literature Session
M2 Takeuchi Aoi

Contents

- **Introduction**

- **Recognition mechanism and preferences of hItln-1 to saccharides**

Wesener, D. A.; Wangkanont, K.; McBride, R.; Song, X.; Kraft, M. B.; Hodges, H. L.; Zarling, L. C.; Splain, R. A.; Smith, D. F.; Cummings, R. D.; Paulson, J. C.; Forest, K. T.; Kiessling, L. L. *Nat. Struct. Mol. Biol.* **2015**, *22*, 603.

- **Conformational Analysis of Recognition of hItln-1 to saccharides**

McMahon, C. M.; Isabella, C. R.; Windsor, I. W.; Kosma, P.; Raines, R. T.; Kiessling, L. L. *J. Am. Chem. Soc.* **2020**, *142*, 2386.

Glycans on Cell Surface

glycans coat the cell surface, which is evolutionarily conserved throughout organisms

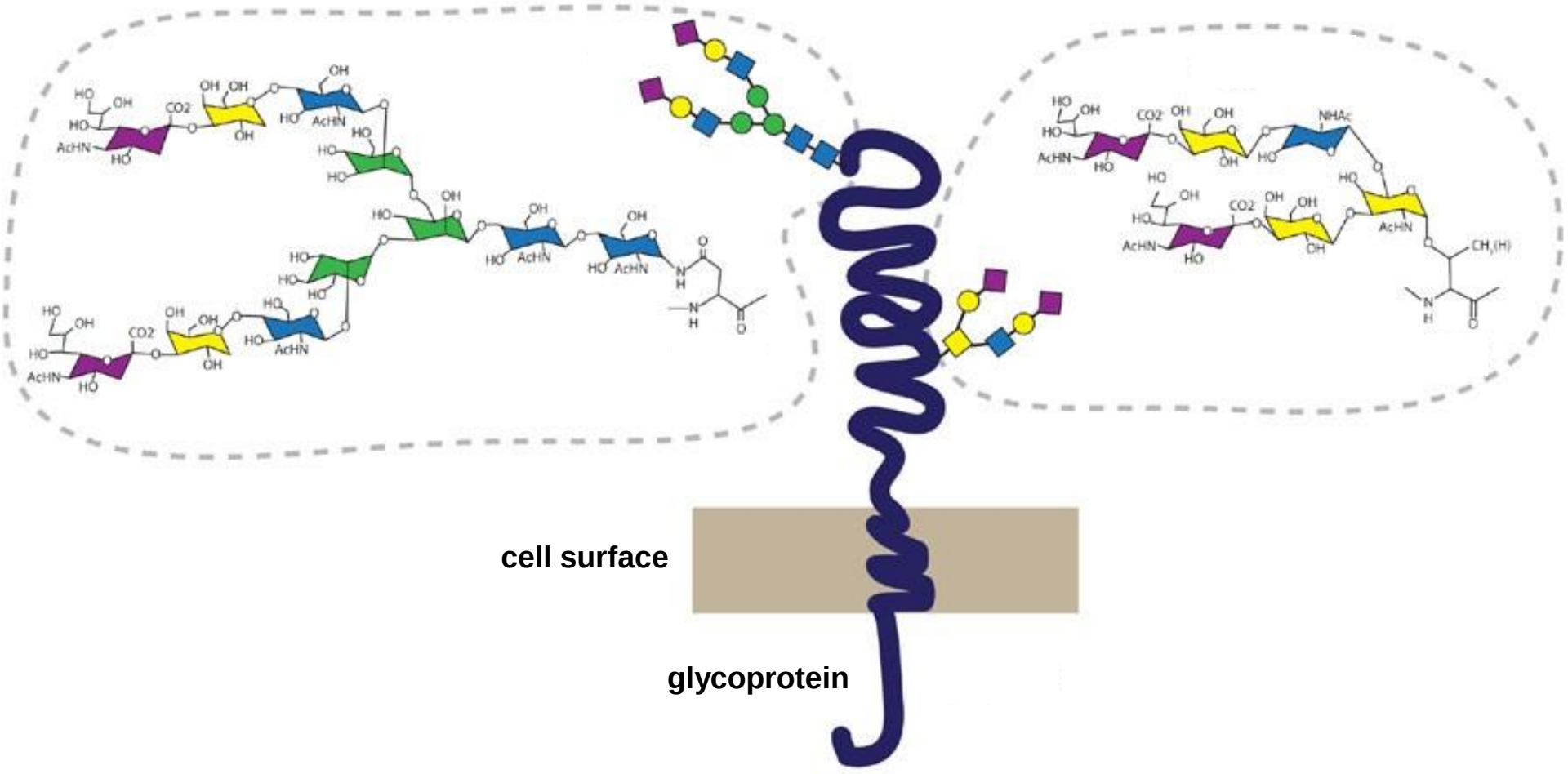

specific recognition of glycans enables a selective targeting to cells of interest, including pathogens

Glycan recognition is a good targeting strategy for therapeutics

Kooyk, Y.; Rabinovich, G. A. *Nat. Immunol.* **2008**, *9*, 593.

Lectin-Glycan Interaction

lectin: carbohydrate-specific proteins that mediate molecular and cellular recognition (<*legere*: select)

glycan

carbohydrate binding determinant

lectin = glycan binding protein

carbohydrate recognition domain (CRD)

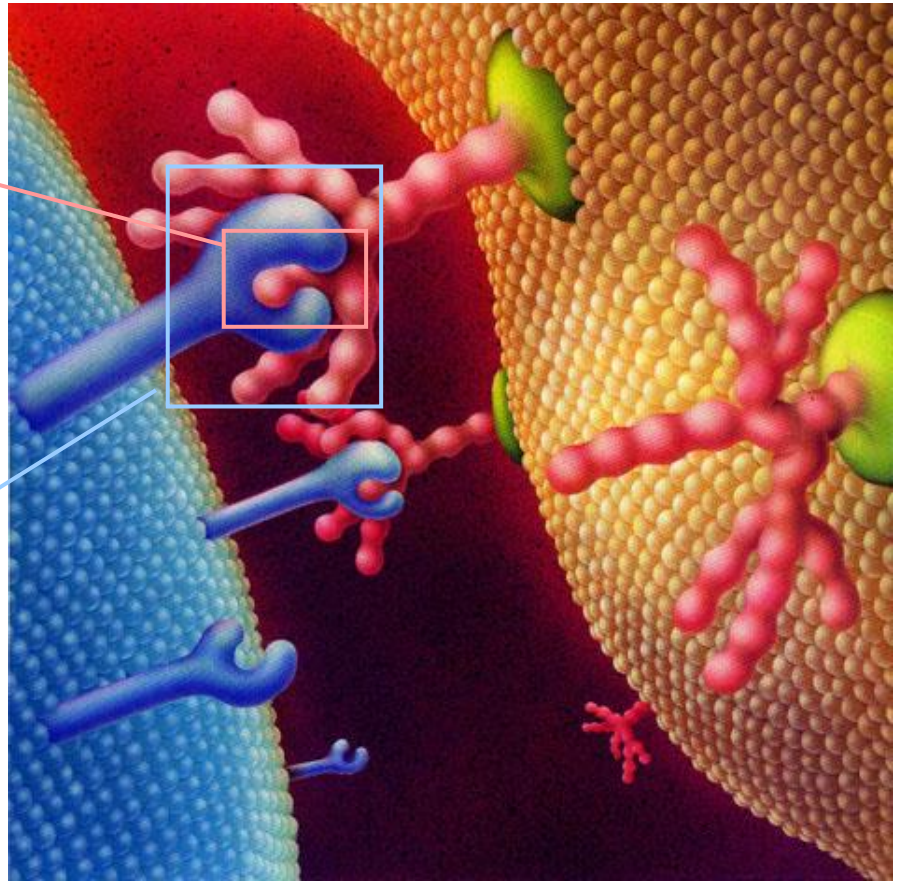

low site affinity (K_D ~ millimolar range), but high multivalent avidity (K_D ~ nanomolar range)
→ combining sugar on cell surfaces, crosslinking of the cells (cell agglutination)

Lectins can selectively target specific cell types by recognizing cell-surface glycans

Lis, H.; Sharon, N. *Chem. Rev.* **1998**, *98*, 637. figure from; Sharon, N.; Lis, H. *Sci. Am.* **1993**, *268*, 82.

Carbohydrate Recognition Mechanisms of Lectin

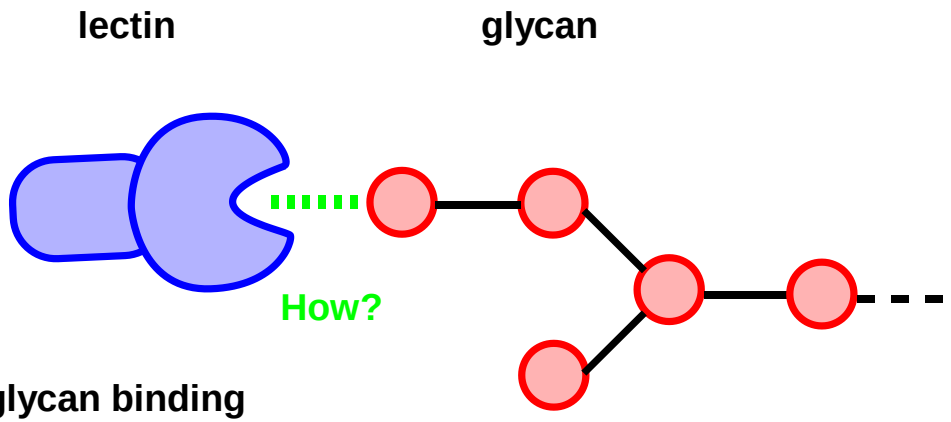

driving force for lectin-glycan binding

- **hydrophobic interaction**
- **solvation effect**

- **hydrogen bonding**

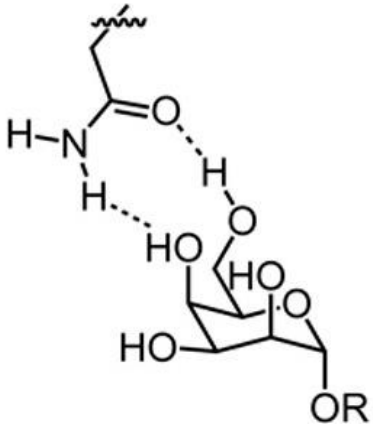

- **CH-π interaction**

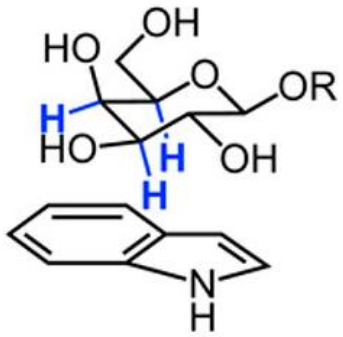

- **metal-mediated binding**

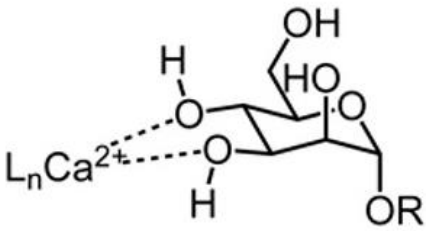

The molecular fundamental principles that govern protein-carbohydrate interactions remain unclear

Kiessling, L. L.; Diehl, R. C. *ACS Chem. Biol.* **2021**, *16*, 1884.; Kiessling, L. L. *Bioorg. Med. Chem.* **2018**, *26*, 5229.

Contents

- Introduction

- **Recognition mechanism and preferences of hItln-1 to saccharides**

Wesener, D. A.; Wangkanont, K.; McBride, R.; Song, X.; Kraft, M. B.; Hodges, H. L.; Zarling, L. C.; Splain, R. A.; Smith, D. F.; Cummings, R. D.; Paulson, J. C.; Forest, K. T.; Kiessling, L. L. *Nat. Struct. Mol. Biol.* **2015**, *22*, 603.

- Conformational Analysis of Recognition of hItln-1 to saccharides

McMahon, C. M.; Isabella, C. R.; Windsor, I. W.; Kosma, P.; Raines, R. T.; Kiessling, L. L. *J. Am. Chem. Soc.* **2020**, *142*, 2386.

Author's Profile

Laura L. Kiessling

- **B.S.: Chemistry, MIT (1983)**
  advised by Prof. Bill Roush
- **Ph.D.: Chemistry, Yale University (1989)**
  advised by Prof. Stuart L. Schreiber
- **Postdoctoral fellow, California Institute of Technology (1989-91)**
  advised by Prof. Peter B. Dervan
- **Steenbock Professor of Chemistry,**
- **Laurens Anderson Professor of Biochemistry**
- **Director of the Keck Center for Chemical Genomics**
  University of Wisconsin-Madison (1991-2017)
- **Novartis Professor of Chemistry, MIT (2017-)**

Focus Areas

elucidating and exploiting interactions on the cell surface,

especially those mediated by proteins binding to carbohydrates

Human Intelectin-1 (hItln-1)

Human intelectin (hItln-1):

- **expressed at mucosal barriers in the small intestine and the lung [1)]**
- **trimeric protein linked with disulfide bonds**
- **has three Ca^{2+} in each monomer (two are buried within the protein, while one is exposed on surface)**
- **binds β-D-galactofuranose (β-Gal*f*) through the Ca^{2+} chelation**

The structure of hItln-1 trimer by X-ray crystallography (as a complex with allyl-β-Gal*f*, PDB ID: 4WMY) [2)]

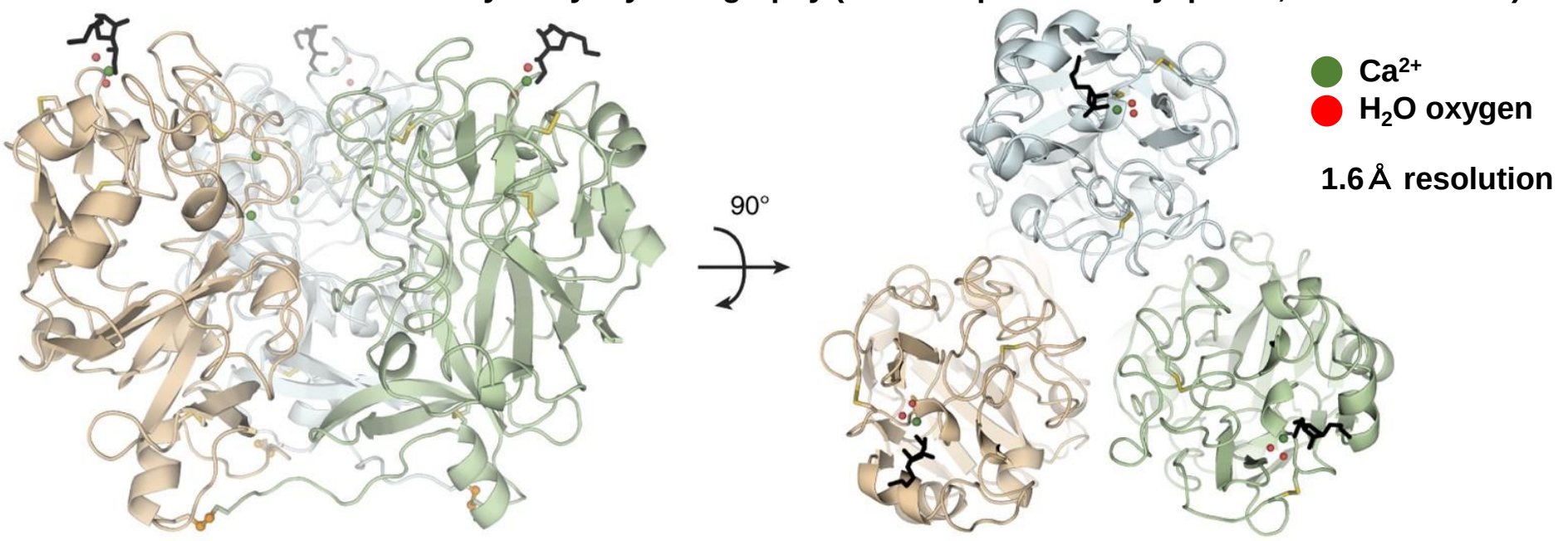

1) a) Suzuki, Y. A.; Shin, K.; Lönnerdal, B. *Biochemistry* **2001**, *40*, 15771.; b) Tsuji, S.; Uehori, J.; Matsumoto, M.; Suzuki, Y.; Matsuhisa, A.; Toyoshima, K.; Seya, T. *J. Biol. Chem.* **2001**, *276*, 23456. c) Voehringer, D.; Stanley, S. A.; Cox, J. S.; Completo, G. C.; Lowary, T. L.; Locksley, R. M. *Exp. Parasitol.* **2007**, *116*, 458.

2) Wesener, D. A.; Wangkanont, K.; McBride, R.; Song, X.; Kraft, M. B.; Hodges, H. L.; Zarling, L. C.; Splain, R. A.; Smith, D. F.; Cummings, R. D.; Paulson, J. C.; Forest, K. T.; Kiessling, L. L. *Nat. Struct. Mol. Biol.* **2015**, *22*, 603.

Glycan Selectivity of HItIn-1

glycan microarray [1] : comprehensive assessment of glycan binding proteins–ligand recognition

characterized glycan library

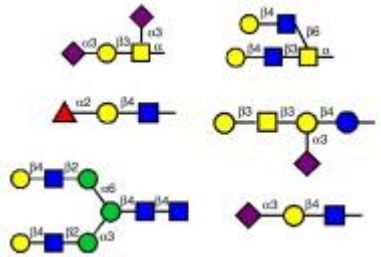

print on a glass slide

incubate with hItIn-1

detect by Alexa Flour 488 labeled IgG

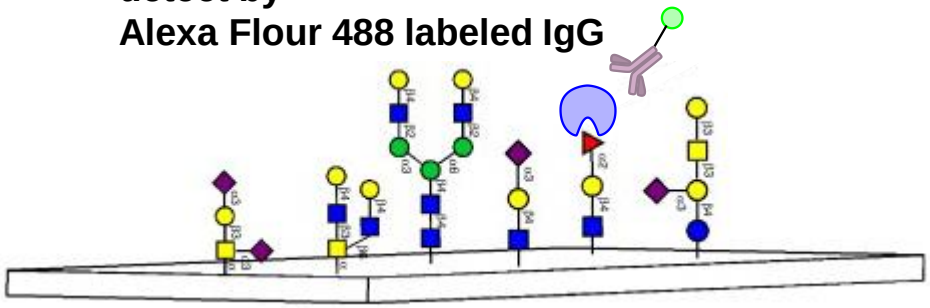

recombinant hItIn-1 binding to (a) mammalian and (b) microbial glycan array [2]

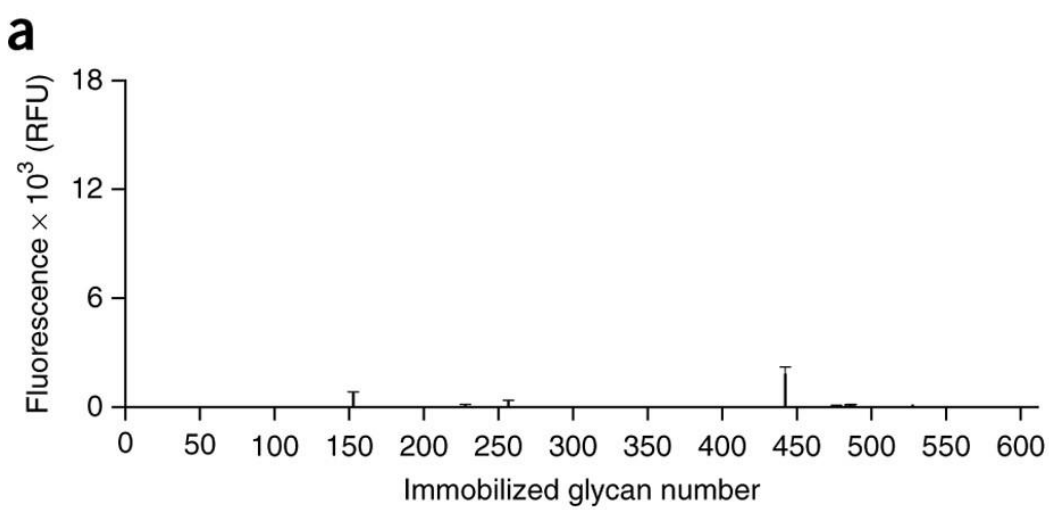

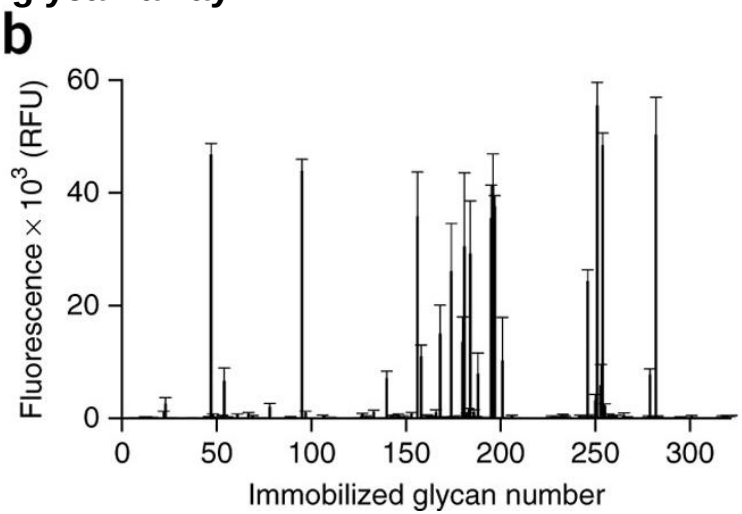

RFU: relative fluorescence units

tested array type: (a) CFG v5.1 array (b) MGMv2

Glycan microarrays demonstrated that hItIn-1 preferentially binded microbial over mammalian glycans

1) Blixt, O.; Head, S.; Mondala, T.; Scanlan, C.; Huflejt, M. E.; Alvarez, R.; Bryan, M. C.; Fazio, F.; Calarese, D.; Stevens, J.; Razi, N.; Stevens, D. J.; Skehel, J. J.; van Die, I.; Burton, D. R.; Wilson, I. A.; Cummings, R.; Bovin, N.; Wong, C. H.; Paulson, J. C. *Proc. Natl. Acad. Sci. U.S.A.* **2004**, *101*, 17033.

2) Wesener, D. A.; Wangkanont, K.; McBride, R.; Song, X.; Kraft, M. B.; Hodges, H. L.; Zarling, L. C.; Splain, R. A.; Smith, D. F.; Cummings, R. D.; Paulson, J. C.; Forest, K. T.; Kiessling, L. L. *Nat. Struct. Mol. Biol.* **2015**, *22*, 603.

Common Epitopes Found in Glycan Ligands

top 15 microbial glycan ligands to hItln-1, sorted by average fluorescence intensity

Rank	Microbial sample	Proposed ligand
1	*S. pneumoniae* type 43	Glycerol phosphate
2	*P. mirabilis* O54ab	Glycerol phosphate
3	*S. pneumoniae* type 56	Glycerol phosphate
4	*P. mirabilis* O54a, 54b	Glycerol phosphate
5	*P. vulgaris* O54a, 54c	Glycerol phosphate
6	*K. pneumoniae* O2a OPS	β-Gal*f*
7	*K. pneumoniae* O2ac OPS	β-Gal*f*
8	*Y. pestis* KM260(11)-Δ0187[a]	
9	*K. pneumoniae* O1 OPS	β-Gal*f*
10	*Y. pestis* 11M-37	Heptose, α-KO, α-KDO
11	*Y. pestis* KM260(11)-6C[a]	
12	*Y. pestis* KM260(11)-Δwaal	Heptose, α-KO, α-KDO
13	*S. pneumoniae* type 20	Heptose, α-KO, α-KDO
14	*Y. pestis* KM260(11)-ΔpmrF	Heptose, α-KO, α-KDO
15	*Y. pestis* 11M-25	Heptose, α-KO, α-KDO

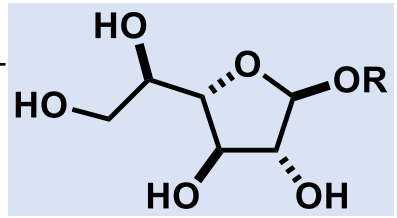

β-D-galactofuranose (β-Gal*f*)

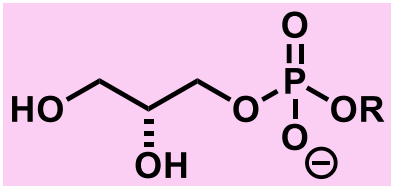

D-glycerol 1-phosphate

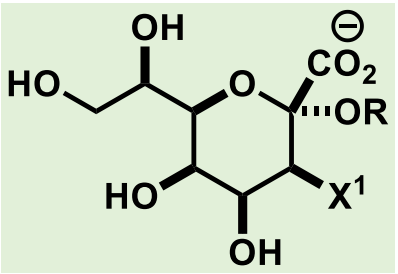

ketooctonic acid (α-KO, X^1 = OH)
ketodeoxyoctonic acid (α-KDO, X^1 = H)

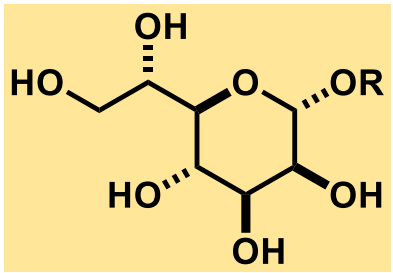

L-*glycero*-α-D-*manno*-heptose

[a] structurally uncharacterized

Good hItln-1 ligands had certain epitopes in common, which are widely distributed in bacteria

Wesener, D. A.; Wangkanont, K.; McBride, R.; Song, X.; Kraft, M. B.; Hodges, H. L.; Zarling, L. C.; Splain, R. A.; Smith, D. F.; Cummings, R. D.; Paulson, J. C.; Forest, K. T.; Kiessling, L. L. *Nat. Struct. Mol. Biol.* **2015**, *22*, 603.

Structural Analysis of Carbohydrate-Binding Site

X-ray crystallography revealed that;

- **The terminal vicinal diol served as a coordinating ligand for Ca^{2+} chelation displacing water molecules**
- **W288 and Y297 formed a binding pocket to accommodate a binding saccharide**
  - **suggested to contribute to enhance binding via CH-π interaction[1)]**
  - **act as walls to preclude the binding of more substituted diols**

structure of the carbohydrate-binding site[2)]

Ca^{2+}
H_2O oxygen

apo-hItln-1 (PDB ID: 4WMQ)

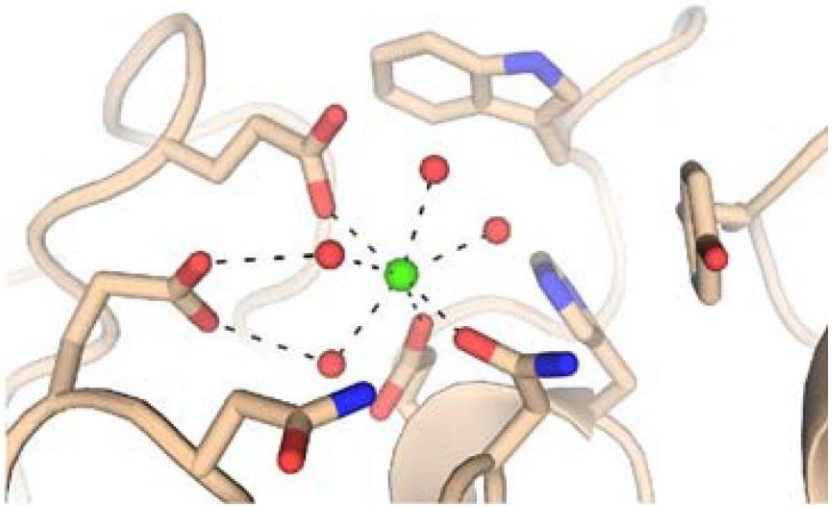

allyl-β-Gal*f*-hItln-1 (PDB ID: 4WMY)

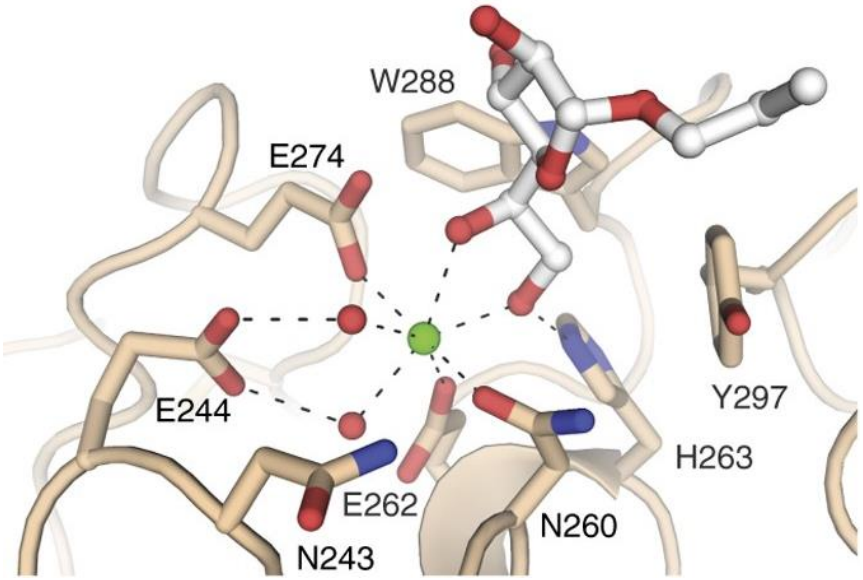

Terminal vicinal diol moiety played a critical role on interaction between hItln-1 and β-Gal*f*

1) Asensio, J. L.; Ardá, A.; Cañada, F. J.; Jiménez-Barbero, J. *Acc. Chem. Res.* **2013**, *46*, 946. 2) Wesener, D. A.; Wangkanont, K.; McBride, R.; Song, X.; Kraft, M. B.; Hodges, H. L.; Zarling, L. C.; Splain, R. A.; Smith, D. F.; Cummings, R. D.; Paulson, J. C.; Forest, K. T.; Kiessling, L. L. *Nat. Struct. Mol. Biol.* **2015**, *22*, 603.

Common Epitopes Found in Glycan Ligands

common feature: terminal vicinal diol

hItln-1 ligands

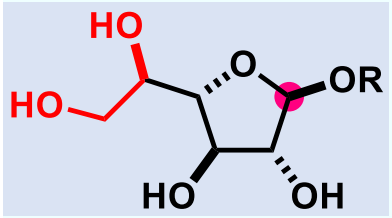

β-D-galactofuranose (β-Gal*f*)

anomeric

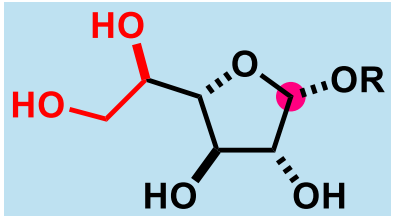

α-D-galactofuranose (α-Gal*f*)

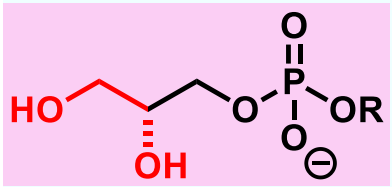

D-glycerol 1-phosphate

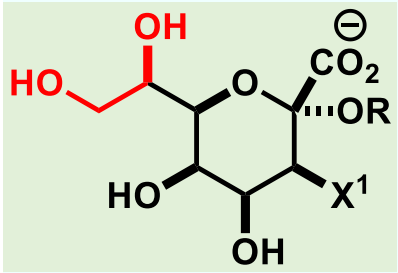

ketooctonic acid (α-KO, X^1 = OH)
ketodeoxyoctonic acid (α-KDO, X^1 = H)

similar

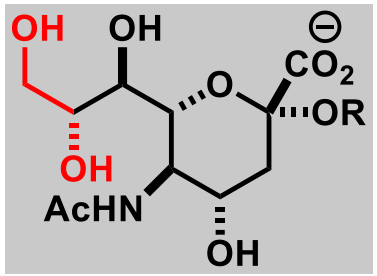

α-*N*-acetylneuraminic acid (α-Neu5Ac)

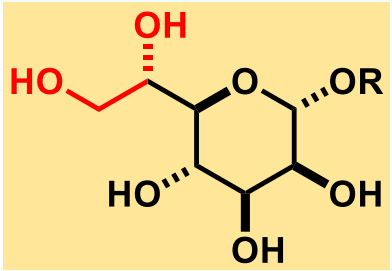

L-*glycero*-α-D-*manno*-heptose

α-Gal*f* or α-Neu5Ac containing glycans <u>failed</u> to bind hItln-1 in the glycan microarray assay

Terminal vicinal diol moiety is necessary but not sufficient for hItln-1 recognition

Wesener, D. A.; Wangkanont, K.; McBride, R.; Song, X.; Kraft, M. B.; Hodges, H. L.; Zarling, L. C.; Splain, R. A.; Smith, D. F.; Cummings, R. D.; Paulson, J. C.; Forest, K. T.; Kiessling, L. L. *Nat. Struct. Mol. Biol.* **2015**, *22*, 603.

Docking Study of α-Neu5Ac and KDO into hItln-1

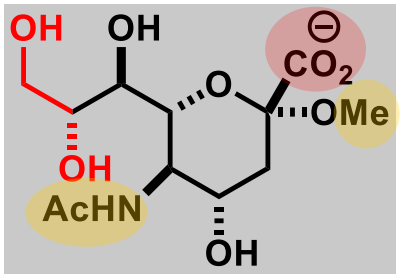

Me-α-Neu5Ac

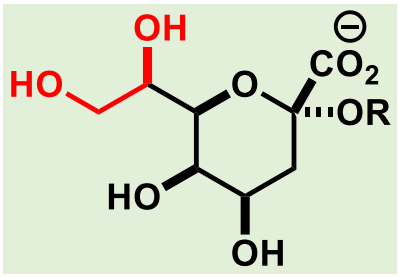

Me-α-KDO

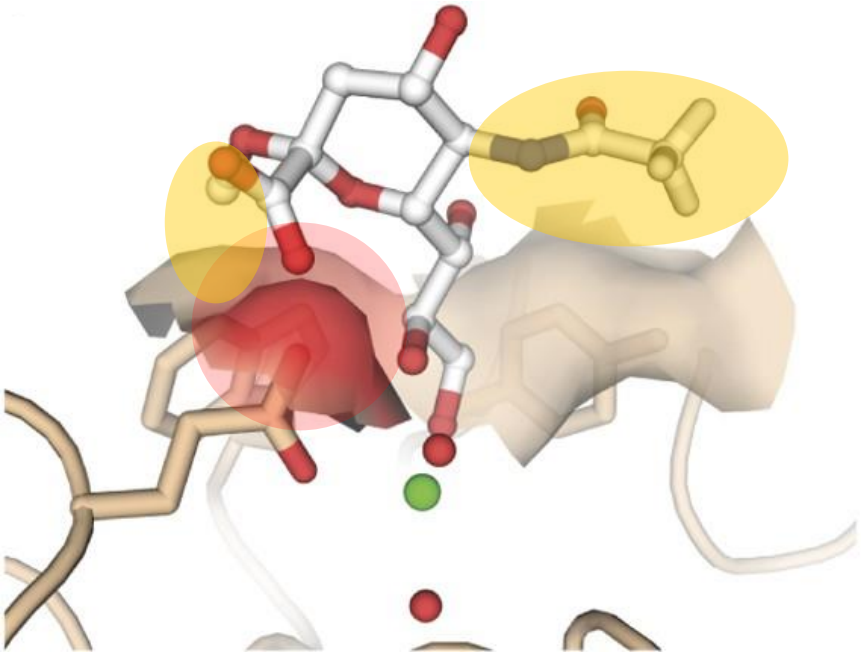

destabilized by **anion-anion repulsion**
steric interaction

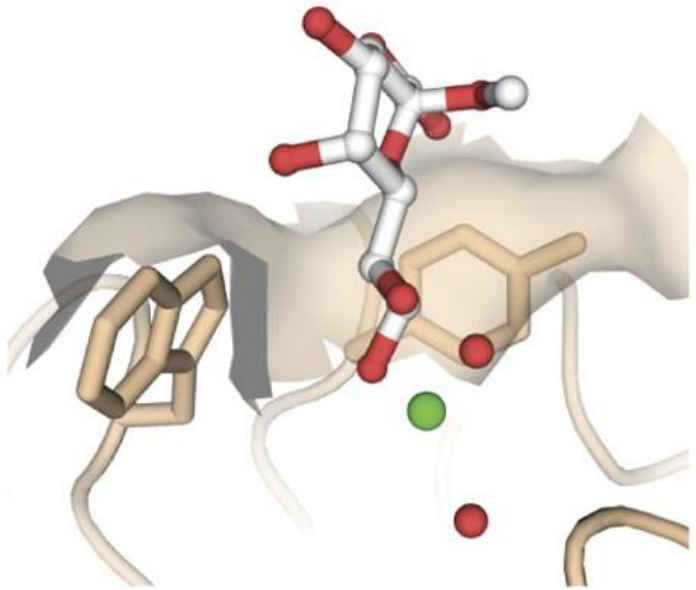

readily accommodated
modeled by PRODRG

- **Several structural properties of glycan contribute to hItln-1 recognition**

➢ **Detailed investigation is necessary for the rationale for hItln-1 selectivity**

Wesener, D. A.; Wangkanont, K.; McBride, R.; Song, X.; Kraft, M. B.; Hodges, H. L.; Zarling, L. C.; Splain, R. A.; Smith, D. F.; Cummings, R. D.; Paulson, J. C.; Forest, K. T.; Kiessling, L. L. *Nat. Struct. Mol. Biol.* **2015**, *22*, 603.

Contents

- **Introduction**

- **Recognition mechanism and preferences of hItln-1 to saccharides**

Wesener, D. A.; Wangkanont, K.; McBride, R.; Song, X.; Kraft, M. B.; Hodges, H. L.; Zarling, L. C.; Splain, R. A.; Smith, D. F.; Cummings, R. D.; Paulson, J. C.; Forest, K. T.; Kiessling, L. L. *Nat. Struct. Mol. Biol.* **2015**, *22*, 603.

- **Conformational Analysis of Recognition of hItln-1 to saccharides**

McMahon, C. M.; Isabella, C. R.; Windsor, I. W.; Kosma, P.; Raines, R. T.; Kiessling, L. L. *J. Am. Chem. Soc.* **2020**, *142*, 2386.

Aim of the Research

microbial saccharides binding hItln-1

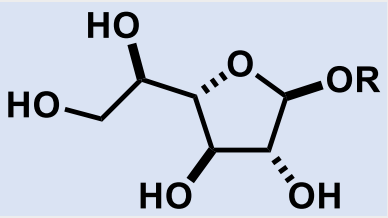

β-D-galactofuranose (β-Gal*f*)

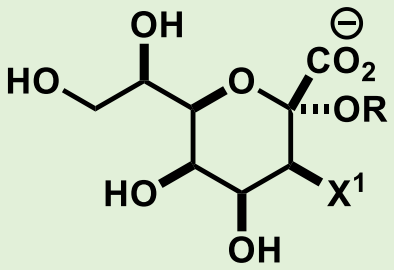

ketooctonic acid (α-KO, X^1 = OH)
ketodeoxyoctonic acid (α-KDO, X^1 = H)

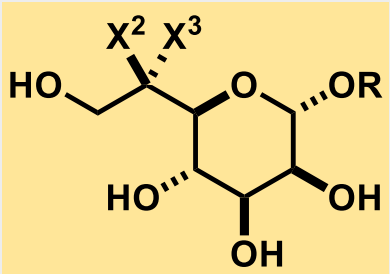

D-*glycero*-α-D-*manno*-heptose (X^2 = OH, X^3 = H)
L-*glycero*-α-D-*manno*-heptose (X^2 = H, X^3 = OH)

specific recognition

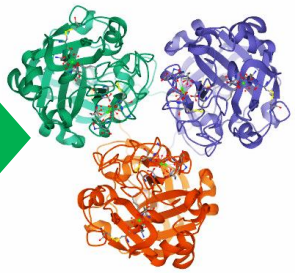

hItln-1

Working hypothesis

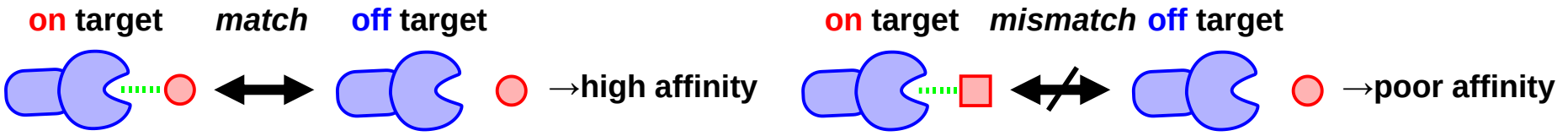

Investigation

hItln-1 binding affinity

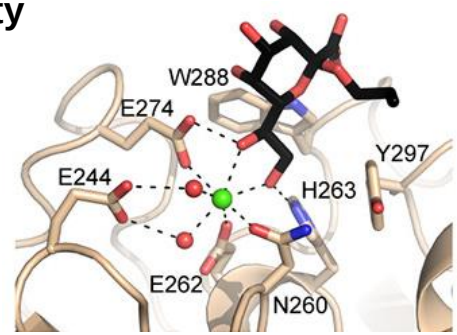

conformational preferences

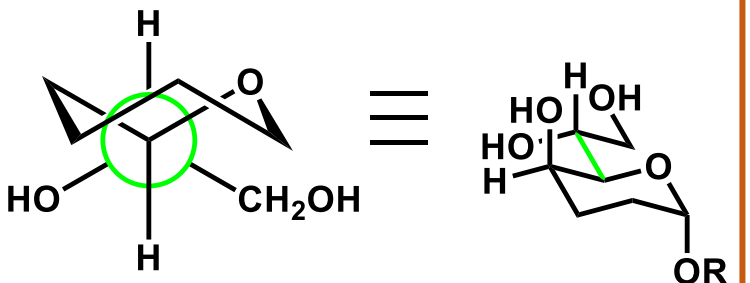

HtIn-1 Binding to Microbial Monosaccharides

	measurement
a. Binding affinity was tested by a competition assay	IC_{50} by BLI
b. Multivalent interactions was tested to understand real cell-surface recognition	K_D by ELISA

a.

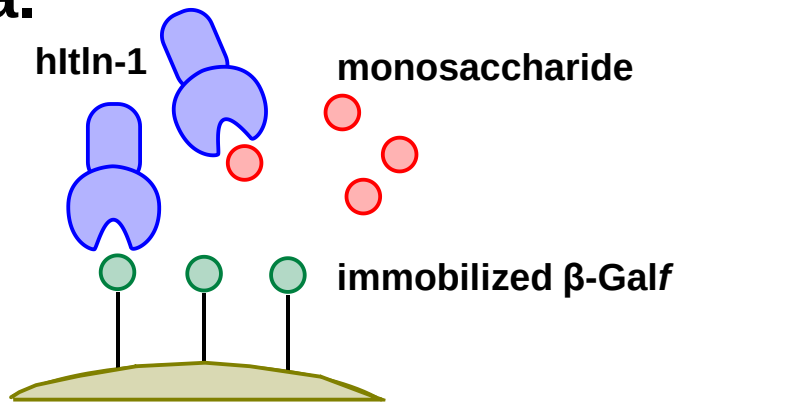

	IC_{50} (mM)	K_D (nM)
α-KO	0.7 (±0.3)	5.1
α-KDO	1.5 (±0.4)	18.3
β-Galf	1.8 (±0.1)	26.2
D,D-heptose	6.8 (±2.3)	-
L,D-heptose	53 (±29)	-

b.

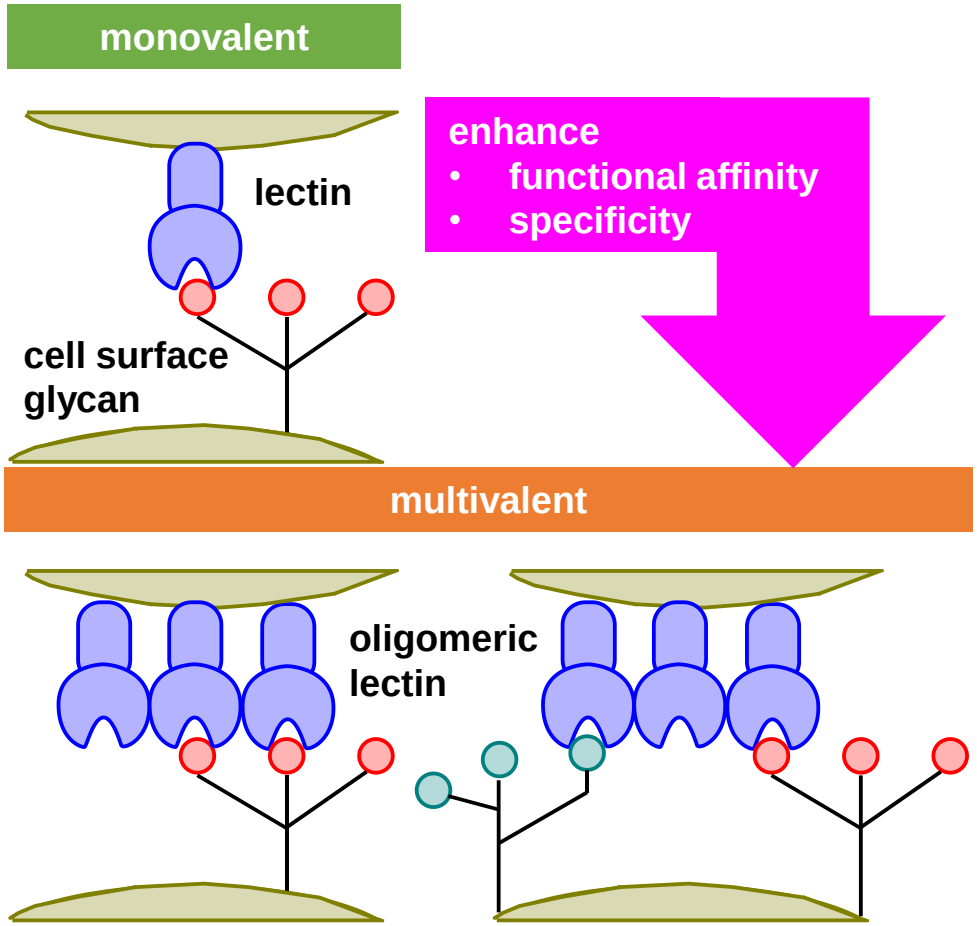

binding affinity: KO, KDO > β-Galf > D,D-heptose, L,D-heptose

Kiessling, L. L.; Grim, J. C. *Chem. Soc. Rev.* **2013**, *42*, 4476.

Biolayer Interferometry (BLI)

Biolayer interferometry (BLI):
label-free method to analyze biomolecular interaction by measuring the change in thickness of the biolayer

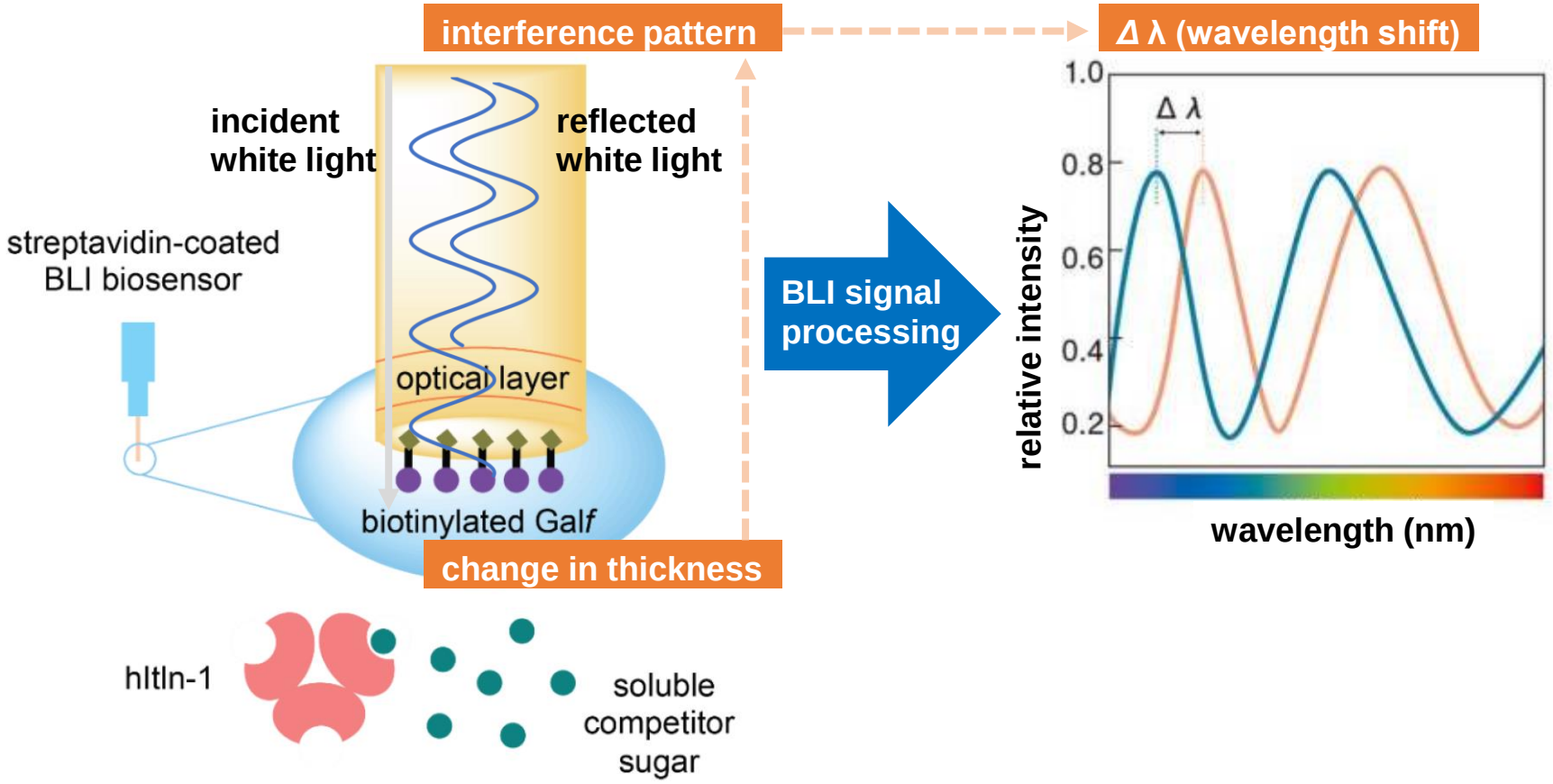

Interference pattern allows for real-time monitoring of molecular interactions on the biosensor surface

Rich, R. L.; Myszka, D. G. *Anal. Biochem.* **2007**, *361*, 1.; Nirschl. M.; Reuter, F.; Vörös. J. *Biosensors*, **2011**, *3*, 70.

Parameters Found by Biolayer Interferometry

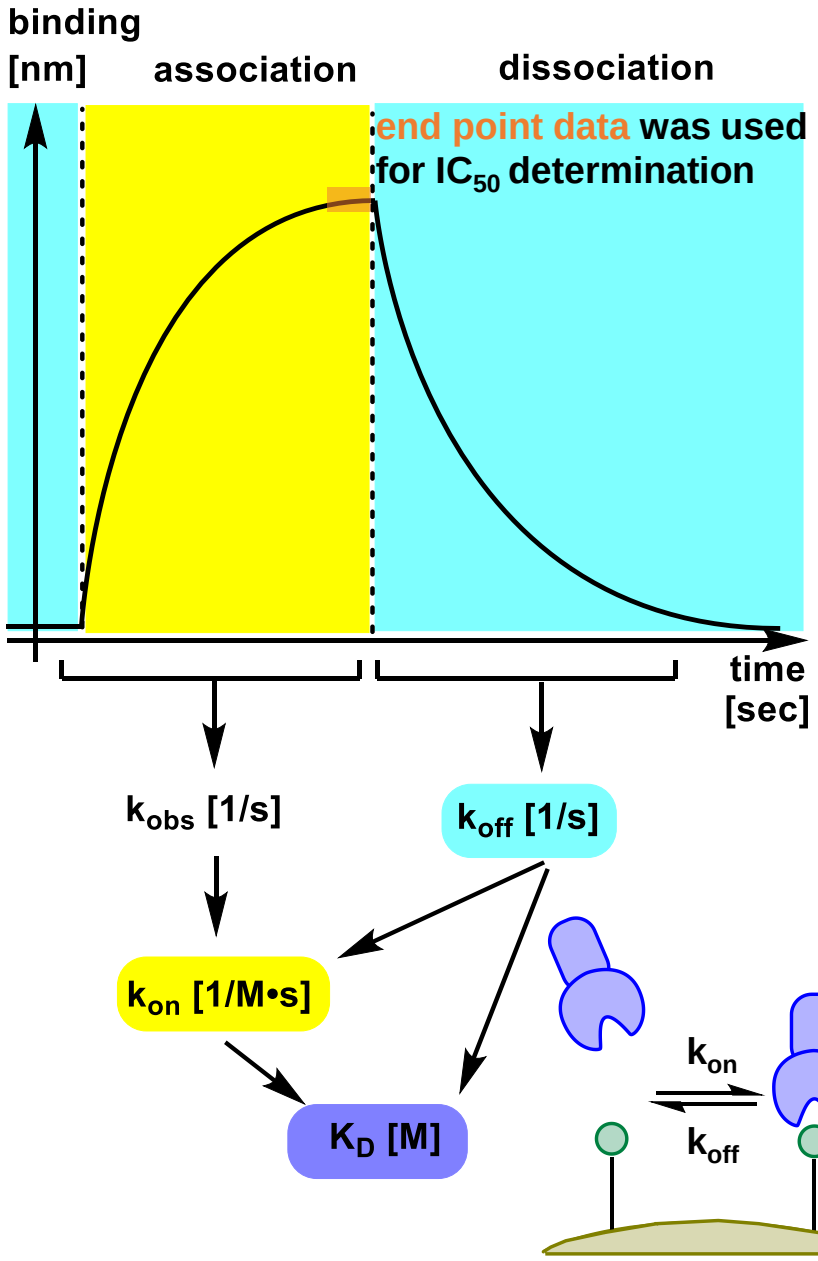

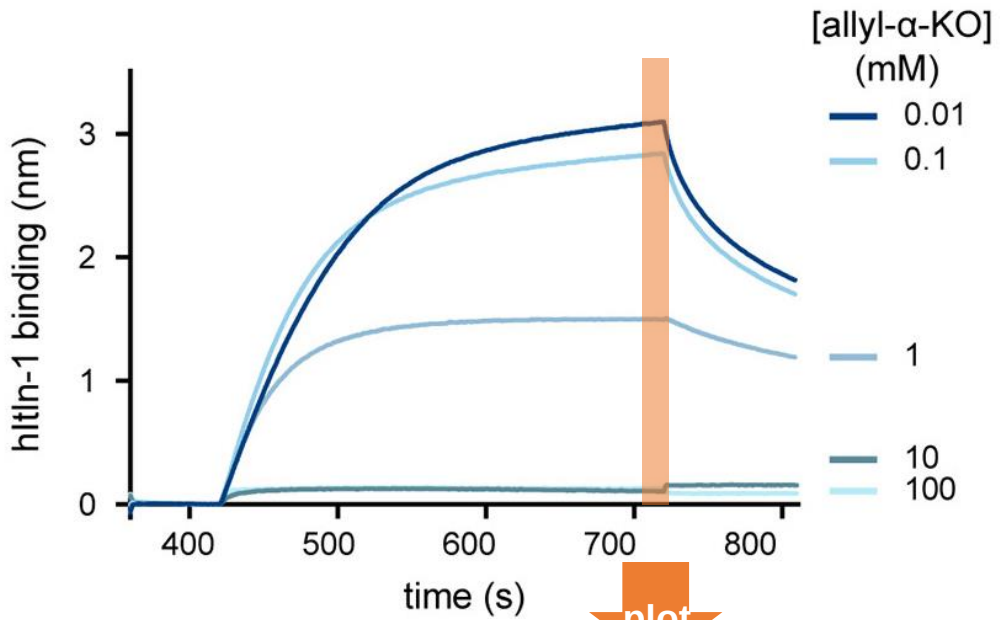

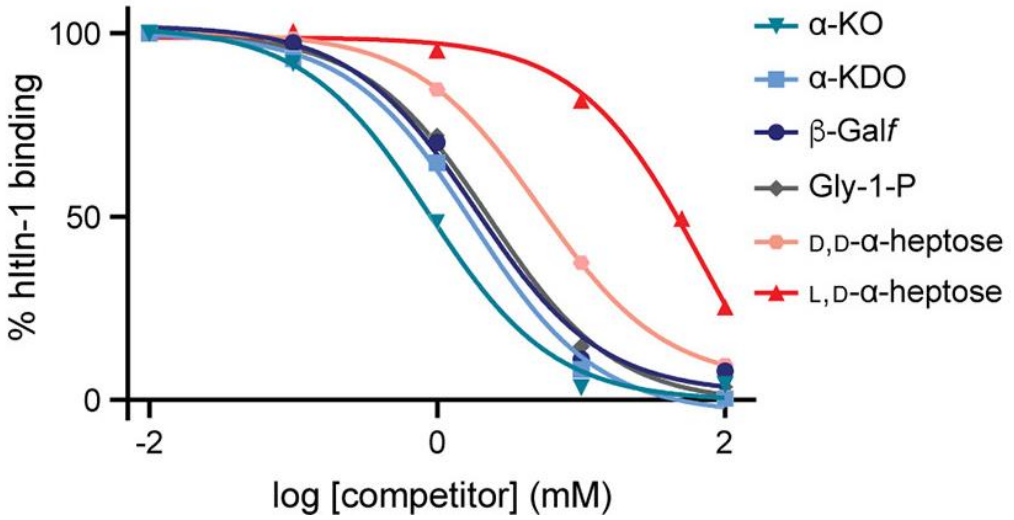

BLI can reveal kinetic constants ($k_{on,off}$), dissociation constants (K_D), and inhibitory concentrations (IC_{50})

Enzyme-linked Immunosorbent Assay (ELISA)

Enzyme-linked immunosorbent assay (ELISA): target molecule utilizing an antigen-antibody reaction
detect/quantify molecule utilizing an enzyme reaction

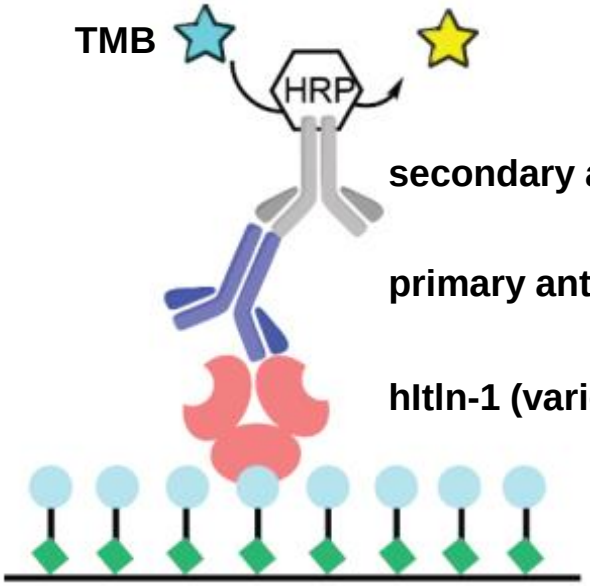

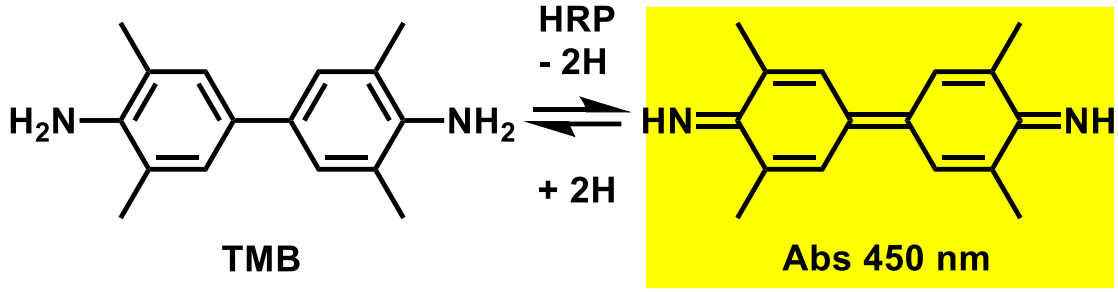

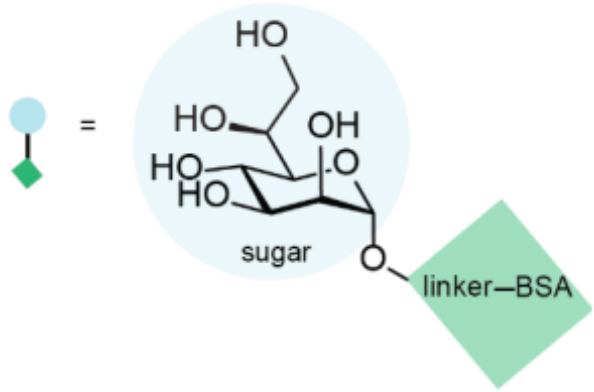

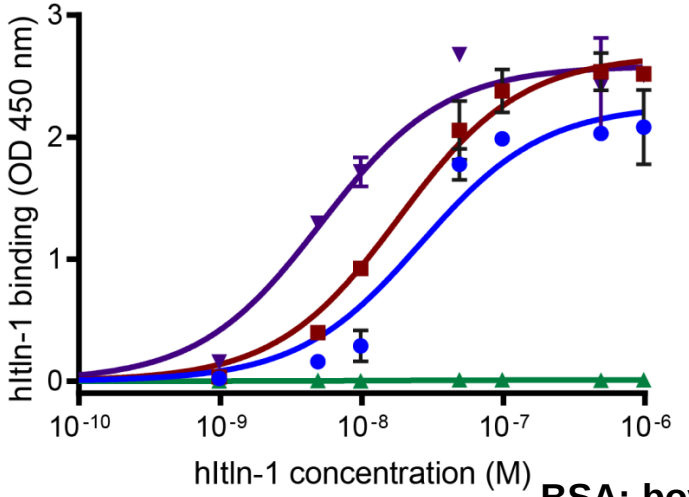

Competitor	K_d (nM)
α-KO-BSA	5.1
α-KDO-BSA	18.3
β-Gal*f*-BSA	26.2
L,D-heptose-BSA	-

BSA: bovine serum albumin
HRP: horseradish peroxidase
TMB: 3,3',5,5'-tetramethylbenzidine
OD: optical density

ELISA can analyze intermolecular interactions with high specificity and quantitatively

Engvail, E; Perlmann, P. *J. Immunol.* **1972**, *109*, 129.

Conformation of the Binding Saccharide

the binding saccharide has three sites of conformational variation

- **proximal rotamer (C_a-C_{a-1} bond)**
- **distal rotamer (C_{a+1}-C_a bond)**

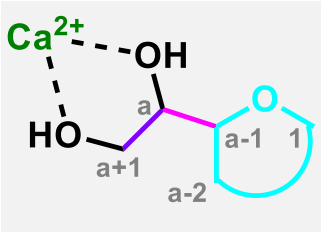

- **ring conformation**
  - **furanose ring (allyl-β-Gal*f*)**
    - **envelope (E) or twisted (T)**
  - **pyranose ring (allyl-α-KO)**
    - **chair (C)**

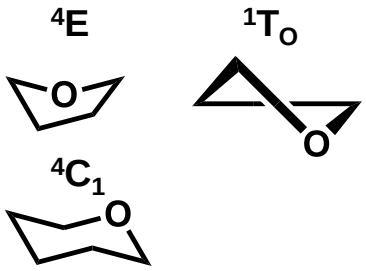

three types of rotamers are named according to the relative orientation of the hydroxyl group
ex) allyl-α-KO proximal rotamer (Newman projection around C_a-C_{a-1} bond)

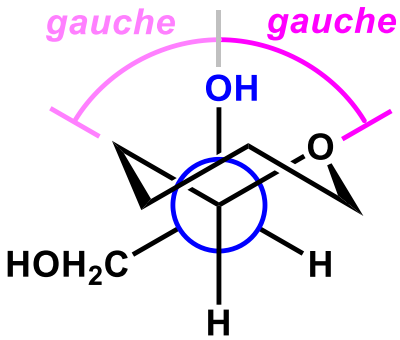

gg

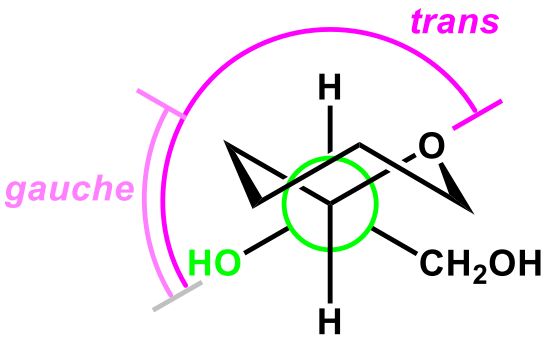

tg

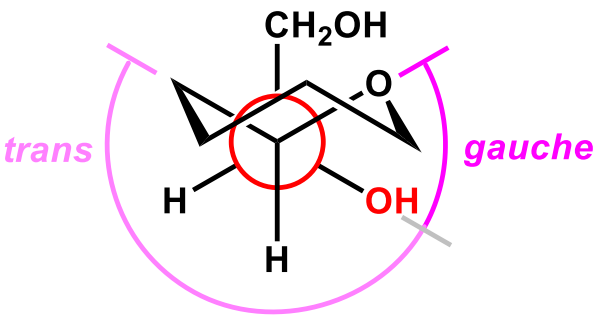

gt

the orientation of the hydroxyl group is listed relative to the C-O bond first, then the C-C bond

proximal rotamer: **C_a-OH relative to C_{a-1}-O, then C_{a-1}-C_{a-2}**
distal rotamer: **C_{a+1}-OH relative to C_a-O, then C_a-C_{a-1}**

3 × 3 = 9 rotamers are possible for the terminal vicinal diol conformation

Richards, M. R.; Bai, Y.; Lowary, T. L. *Carbohydr. Res.* **2013**, *374*, 103.

Conformational Analysis of the Binding Saccharide

allyl-α-KO-hItln-1 (PDB ID: 6USC)

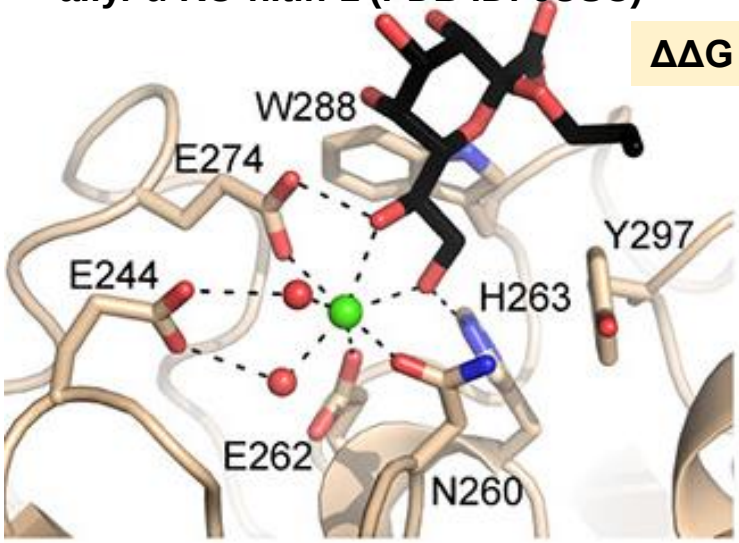

ΔΔG = -0.6 kcal/mol[a]

allyl-β-Gal*f*-hItln-1 (PDB ID: 4WMY)

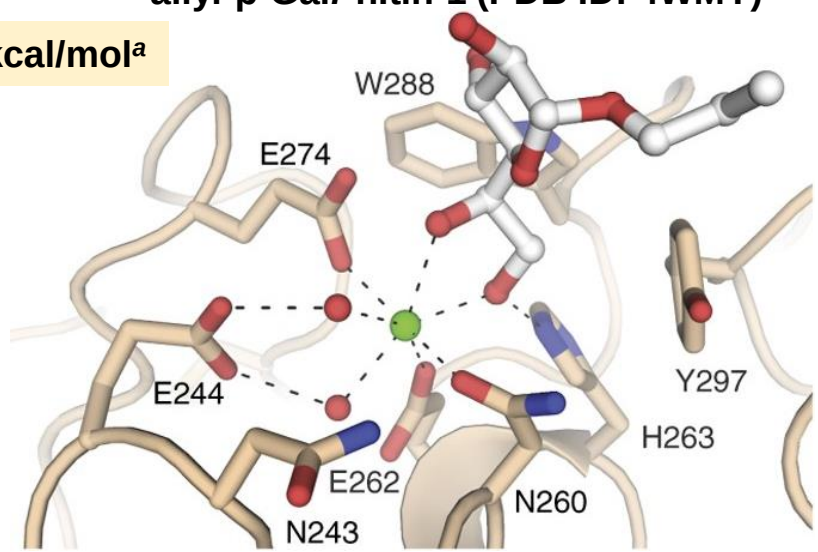

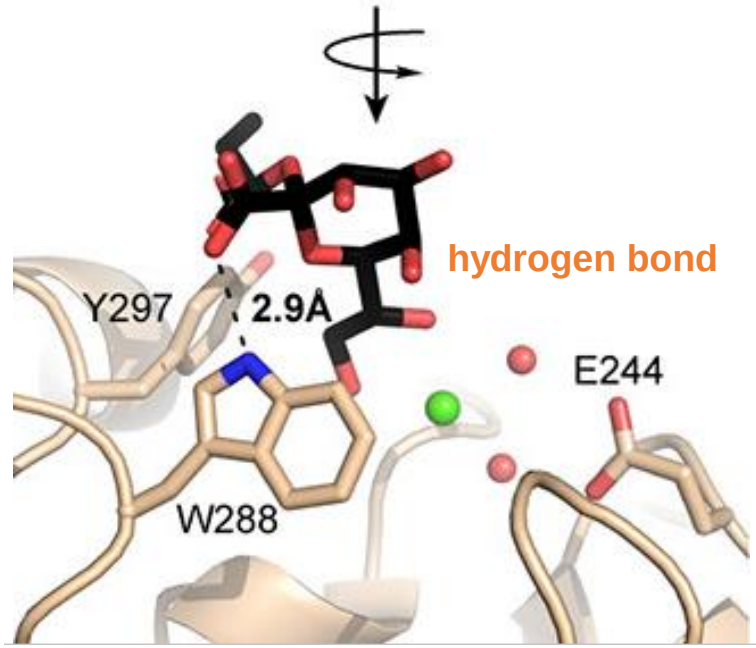

Ca^{2+}
H_2O oxygen

allyl-α-KO conformation: *tg*-*gt*
allyl-β-Gal*f* conformation: *gg*-*gt*

[a] estimated from IC_{50} by BLI competition assay

- **Ca^{2+} coordination by a saccharide demands that the two hydroxyl groups of the vicinal diol are *gauche***
- **Additional hydrogen bond could contribute to the higher affinity for α-KO over β-Gal*f***

Wesener, D. A.; Wangkanont, K.; McBride, R.; Song, X.; Kraft, M. B.; Hodges, H. L.; Zarling, L. C.; Splain, R. A.; Smith, D. F.; Cummings, R. D.; Paulson, J. C.; Forest, K. T.; Kiessling, L. L. *Nat. Struct. Mol. Biol.* **2015**, *22*, 603.

Bioinformatic Search of Glycan Conformation

Which conformation do glycans generally adopt when they bind to lectins?

× sialic acid
× incomplete electron density
× covalent linkage

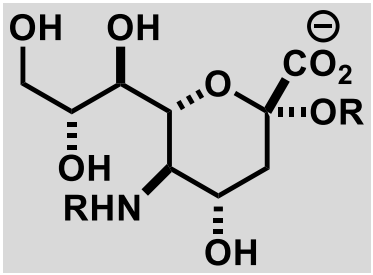

exclude

lectin-ligand structures in Protein Data Bank (PDB)

searched structure (ligand):
pyranose with exocyclic vicinal diol at C_5
furanose with exocyclic vicinal diol at C_4
resolution: ≤ 2.0 Å

97 structures

67 structures

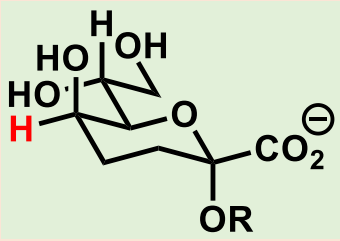

pyranose
with equatorial H at C_5
(KO/KDO-like)

24 structures

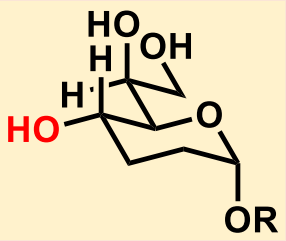

pyranose
with equatorial OH at C_4
(heptose-like)

6 structures

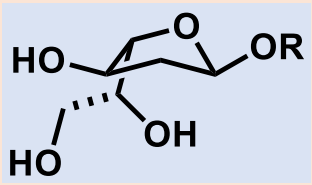

furanose
(Gal*f*-like)

Hit structures were categorized into 3 patterns based on a ligand similarity

Bioinformatic Analysis of Glycan Conformation

KO/KDO-like

67 hits		proximal rotamer *gg*	proximal rotamer *tg*	proximal rotamer *gt*
distal rotamer	*gg*	0	34	0
	tg	2	2	0
	gt	0	29	0

heptose-like

24 hits		proximal rotamer *gg*	proximal rotamer *tg*	proximal rotamer *gt*
distal rotamer	*gg*	0	0	0
	tg	2	0	0
	gt	19	0	3

Gal*f*-like

6 hits		proximal rotamer *gg*	proximal rotamer *tg*	proximal rotamer *gt*
distal rotamer	*gg*	1	0	0
	tg	3*	0	0
	gt	2*	0	1

*** one structure showed alternate conformations with distal OH in *tg* and *gt***

most prevalent conformation **

L,D-heptose

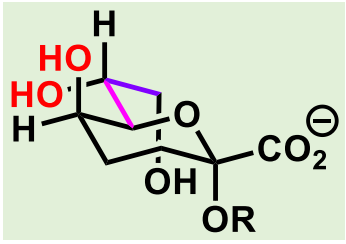

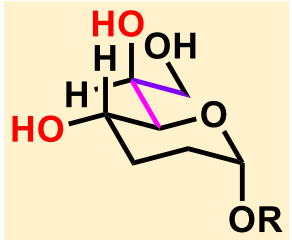

D,D-heptose[1)]

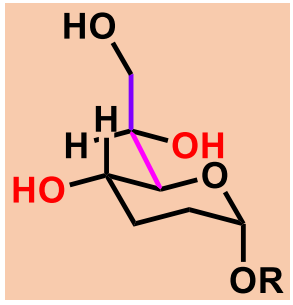

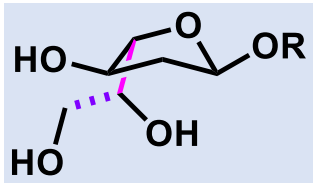

**** ring hydroxyl groups were omitted for clarity**

- **Searched saccharides shared a strong conformational preference in the proximal rotamer**
- **The configuration of hydroxyl groups dramatically affected the prevalent conformation**

1) Wang, H.; Head, J.; Kosma, P.; Brade, H.; Müller-Loennies, S.; Sheikh, S.; McDonald, B.; Smith, K.; Cafarella, T.; Seaton, B.; Crouch, E. *Biochemistry* **2008**, *47*, 710.

Conformational Preference and Binding Affinity

Working hypothesis

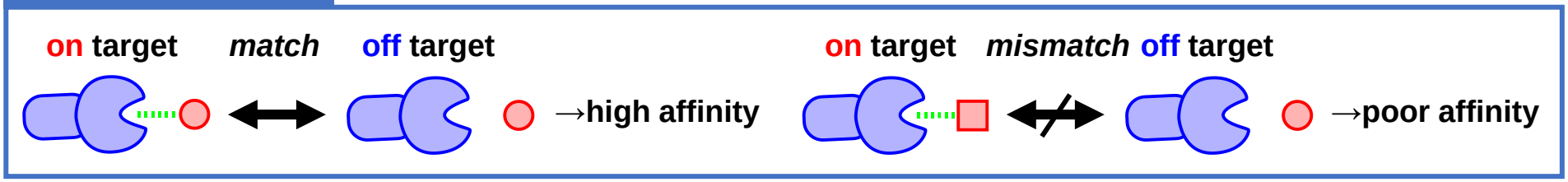

α-KO — D,D-heptose — L,D-heptose

binding affinity to hItIn-1: high ⟷ poor

accommodated conformation on interaction with hItIn-1

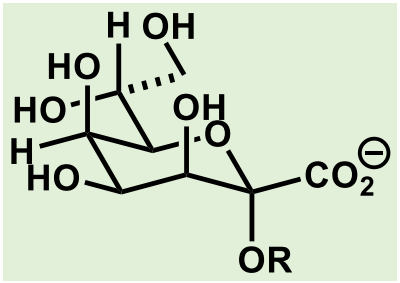

tg-gt (by X-ray)

? ? docking study

match/ mismatch | *match/ mismatch* | *match/ mismatch*

low-energy conformation off interaction with hItIn-1

? ? ? natural bond orbital (NBO) analysis

Docking Study of Side Chain Conformation

structures of L,D-, D,D-heptoses bound to surfactant protein D[1)] (PDB ID: 2RIB, 2RIA)

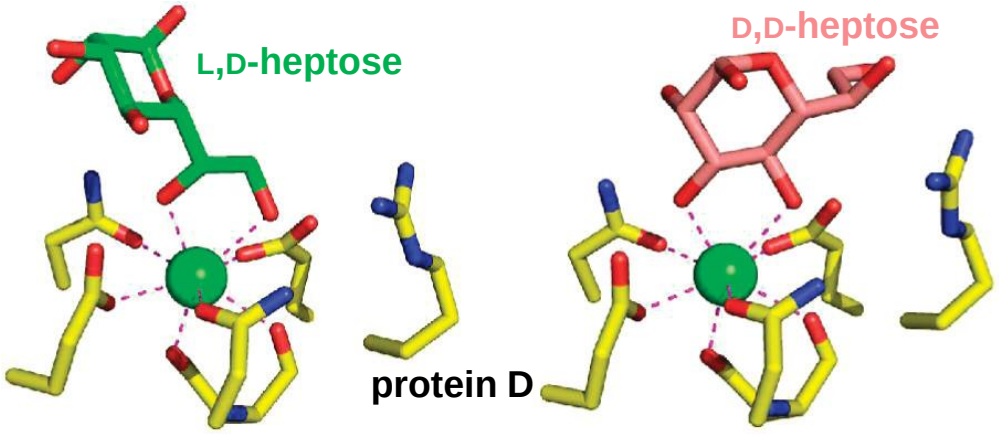

structure of allyl-α-KO bound to hItln-1 (PDB ID: 6USC)

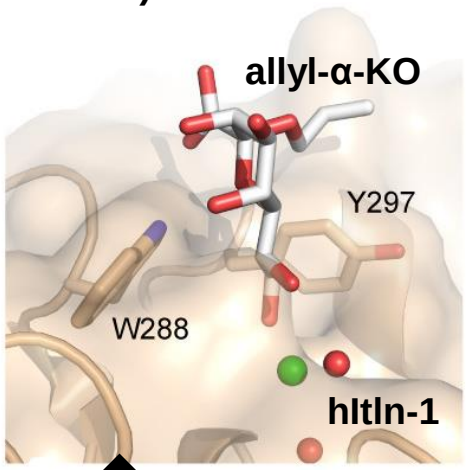

1. extract coordinates

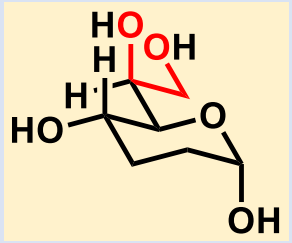

gg-*gt*

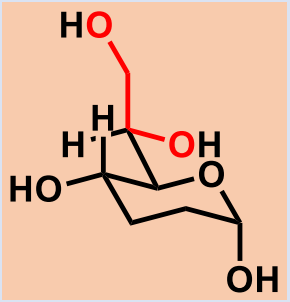

gt-*gt*

2. align vicinal diol

3. substitute for allyl-α-KO

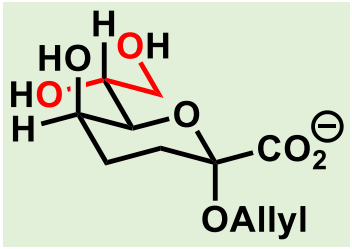

tg-*gt*

The prevalent conformations of heptoses were simulated on hItln-1 binding site

1) Wang, H.; Head, J.; Kosma, P.; Brade, H.; Müller-Loennies, S.; Sheikh, S.; McDonald, B.; Smith, K.; Cafarella, T.; Seaton, B.; Crouch, E. *Biochemistry* **2008**, *47*, 710.

Accommodated Conformation of Heptoses

most prevalent conformation	accommodated conformation

L,D-heptose

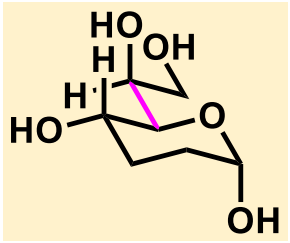

gg-*gt*

steric repulsion

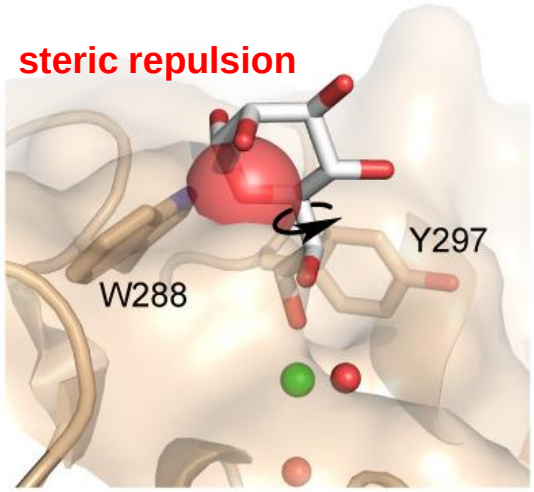

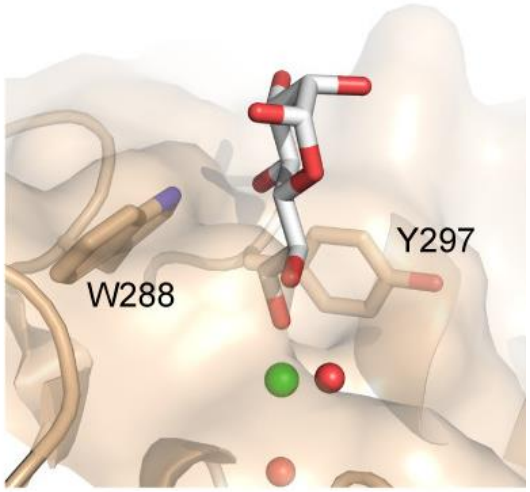

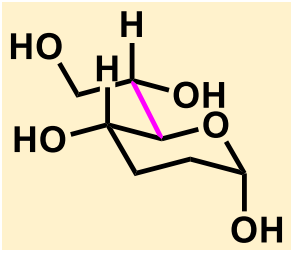

gt-*gt*

D,D-heptose

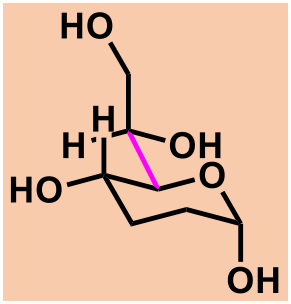

gt-*gt*

steric repulsion

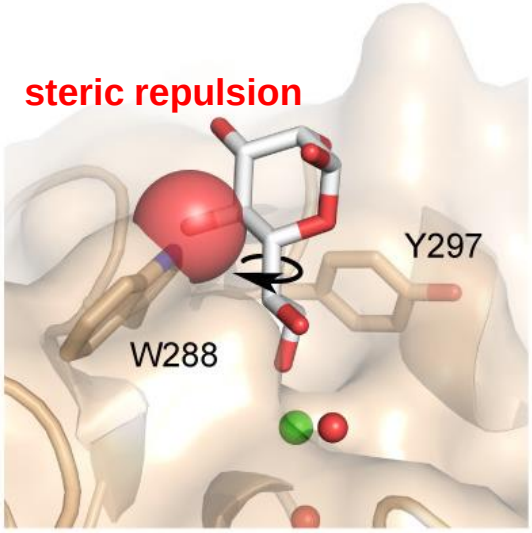

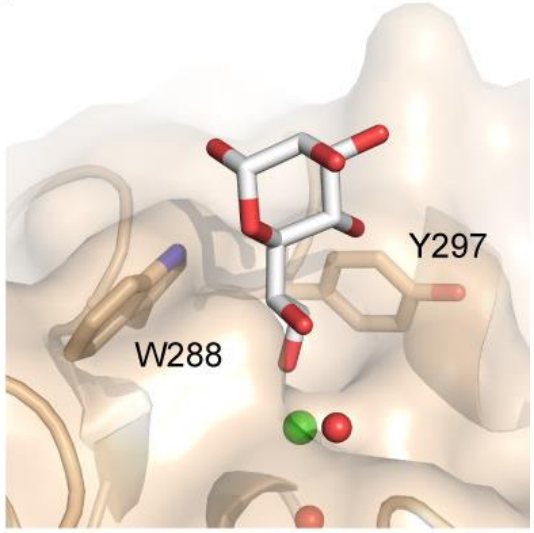

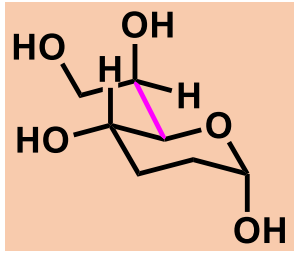

gg-*gt*

- The most prevalent conformations of L,D-, D,D-heptoses did not fit the binding site of hItln-1

Natural Bond Orbital (NBO) Analysis

The stability of the conformation could be discussed by anomeric interaction

C-O bond is electron deficient ($n_O \rightarrow \sigma^*_{C\text{-}O}$, inductive effect)

stabilized ← **$\sigma_{C\text{-}H} \rightarrow \sigma^*_{C\text{-}O}$ donation**

allyl-α-KO
equatorial C_5-H

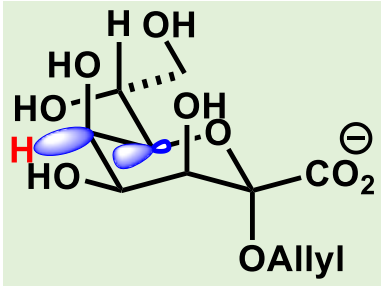

donation from C_5-H

allyl-L,D-heptose
axial C_4-H

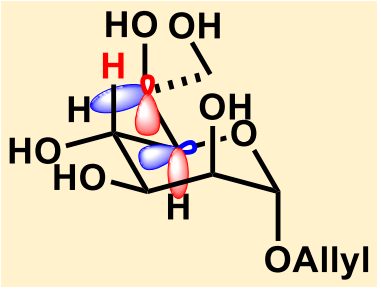

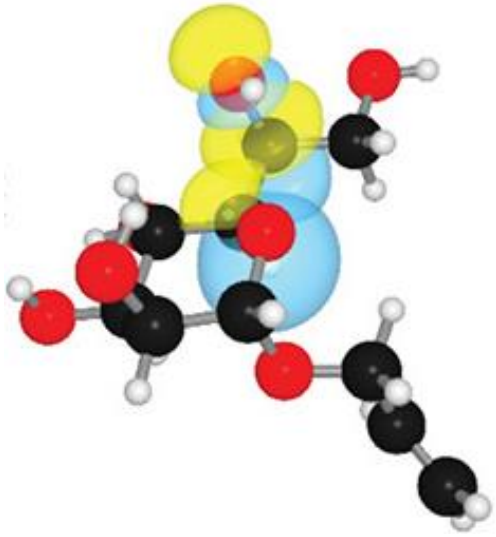

~~**donation from C_4-H**~~

donation from side chain C_6-H

stabilization from $\sigma_{C5\text{-}H} \rightarrow \sigma^*_{C6\text{-}O}$

low-energy conformation: *tg*-*gt*
☑ **steric preference**

low-energy conformation: *gg*-*gt*
☑ **hyperconjugation**

blue, yellow orbitals: NBO renderings of significant $\sigma_{C\text{-}H} \rightarrow \sigma^*_{C\text{-}O}$ interactions
level of theory: M06-2X/6-311+G(d,p)
solvation model: IEFPCM

The prevalent conformation would be stabilized by hyperconjugation

Stereoelectronic Effect on Heptane Conformation

low-energy conformation of heptose: determined by **stereoelectronic stabilization** and **steric destabilization**

allyl-D,D-heptose

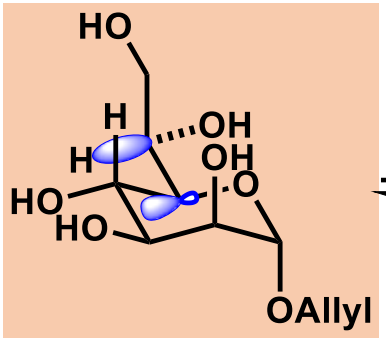

gt-*gt*

$\sigma_{C6\text{-}H} \rightarrow \sigma^*_{C5\text{-}O}$

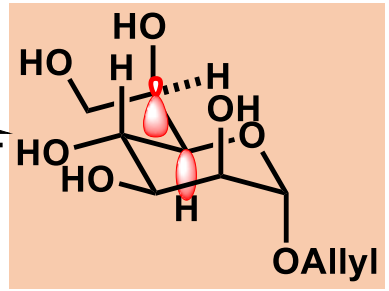

gg-*gt*

$\sigma_{C5\text{-}H} \rightarrow \sigma^*_{C6\text{-}O}$

syn-pentane interaction

low-energy conformation: *gt*-*gt*
ΔE_{NBO} = 0.19 kcal/mol

allyl-L,D-heptose

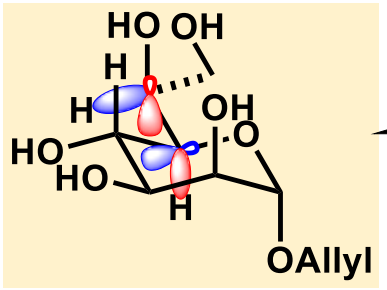

gg-*gt*

$\sigma_{C6\text{-}H} \rightarrow \sigma^*_{C5\text{-}O}$

$\sigma_{C5\text{-}H} \rightarrow \sigma^*_{C6\text{-}O}$

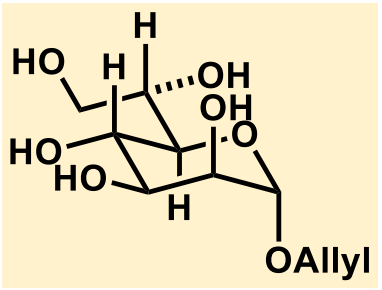

gt-*gt*

syn-pentane interaction

low-energy conformation: *gg*-*gt*
ΔE_{NBO} = 3.25 kcal/mol

ΔE_{NBO}: NBO donor-acceptor energy
level of theory: M06-2X/6-311+G(d,p)
solvation model: IEFPCM

- NBO analysis indicated that the prevalent conformations in PDB are in the lowest-energy
- Less ΔE_{NBO} of allyl-D,D-heptose is consistent with the binding affinity: D,D-heptose > L,D-heptose

Summary

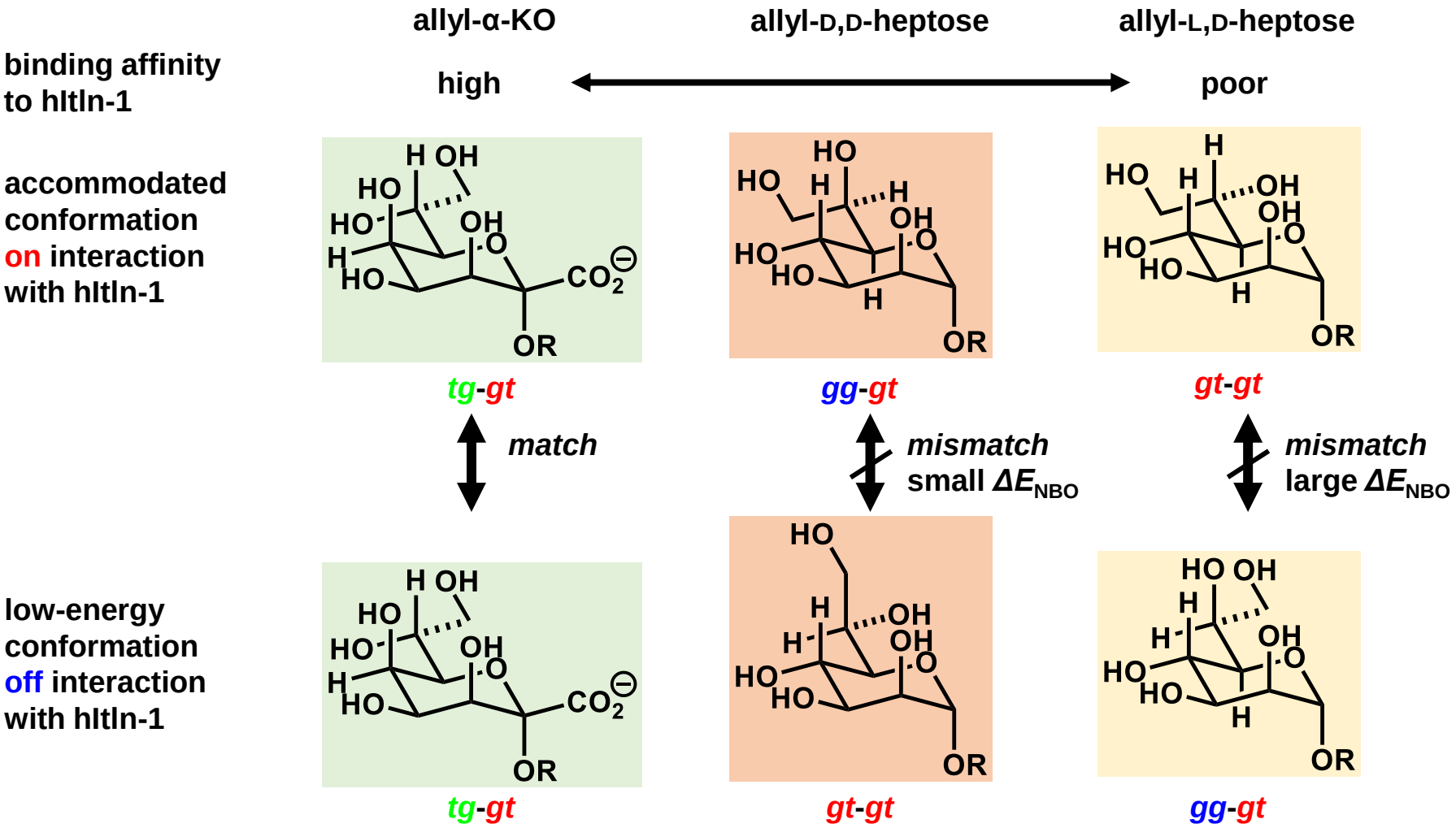

- The relationship between the binding affinity and the conformational preference was investigated about several microbial saccharides binding to hItln-1
- The binding of a saccharide to hItln-1 is dominated by the vicinal diol conformation
- This study pioneered a conformational analysis toward understanding of lectin-glycan interactions

Exceptional Structure found in Conformation Search

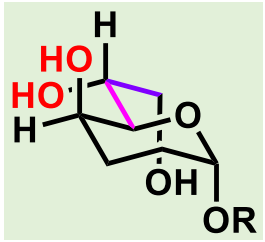

KO/KDO-like

67 hits		proximal rotamer gg	tg	gt
distal rotamer	gg	0	34	0
	tg	2	2	0
	gt	0	29	0

OmpE36-LPS complex

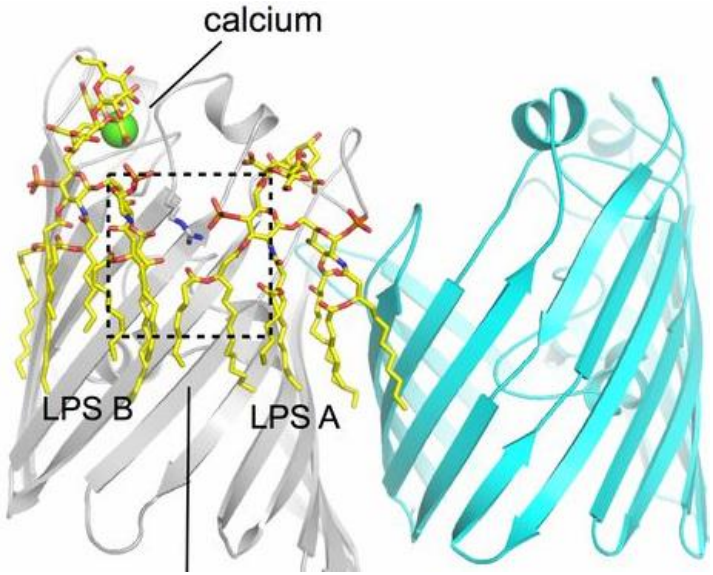

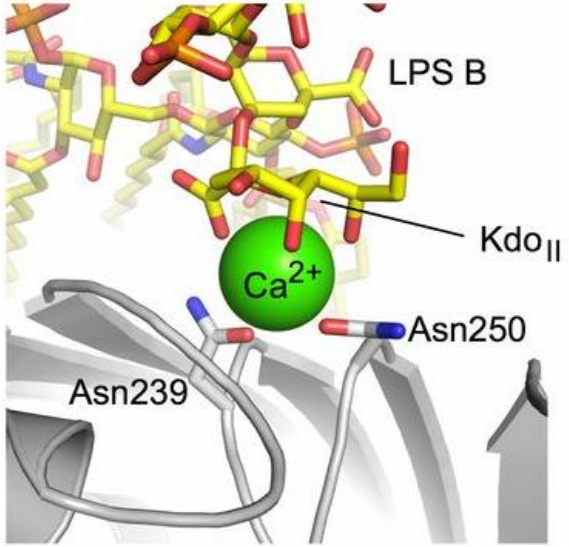

LPS: Lipopolysaccharides
OMP: outer membrane proteins of gram-negative bacteria

The aberrant preference was driven by the simultaneous coordination of KDO carboxylate and the axial hydroxyl and C7 side chain hydroxyl groups to Ca^{2+}

Arunmanee, W.; Pathania, M.; Solovyova, A. S.; Le Brun, A. P.; Ridley, H.; Baslé, A.; van den Berg, B.; Lakey, J. H. *Proc. Natl. Acad. Sci. U. S. A.* **2016**, *113* (34), E5034

Exceptional Structure found in Conformation Search

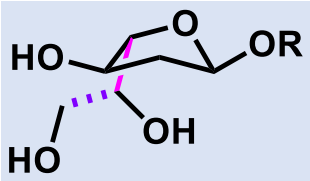

Gal*f*-like

6 hits		proximal rotamer *gg*	*tg*	*gt*
distal rotamer	*gg*	1	0	0
	tg	3*	0	0
	gt	2*	0	1

Binding site of YtfQ containing both α- and β-Gal*f*

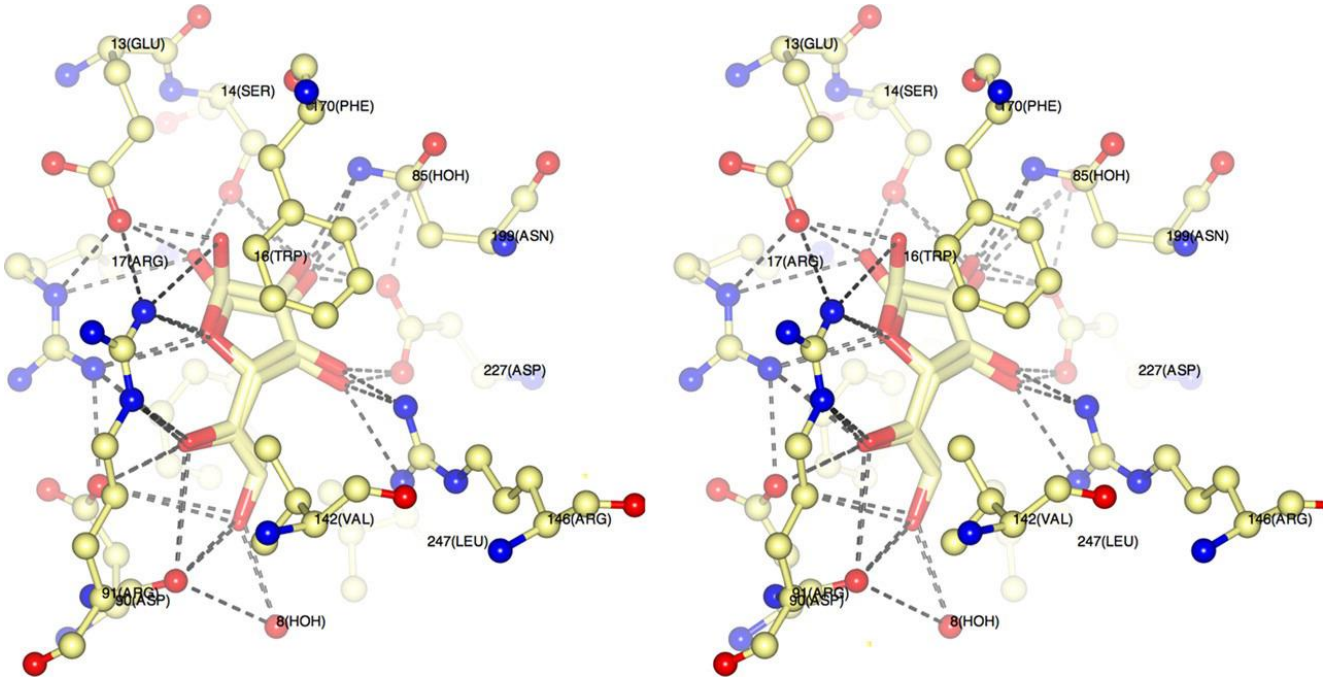

YtfQ: a kind of a sugar ABC transporter of *E*. Coli encoded by *ytfQRTyjfF* operon

three hydrogen bonds involving the proximal hydroxyl group, likely influencing the conformation

Horler, R. S. P.; Müller, A.; Williamson, D. C.; Potts, J. R.; Wilson, K. S.; Thomas, G. H. *J. Biol. Chem.* **2009**, *284*, 31156.

Ring Conformational Analysis of the Binding β-Gal*f*

two hItln-1 monomers are present in the asymmetric unit (chain A and chain B)

structural comparison of the crystallized allyl-β-Gal*f* ligands

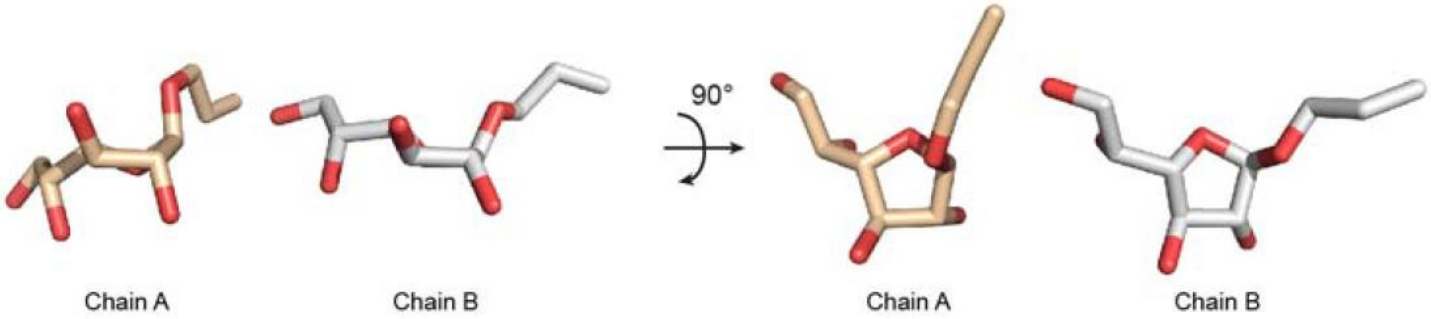

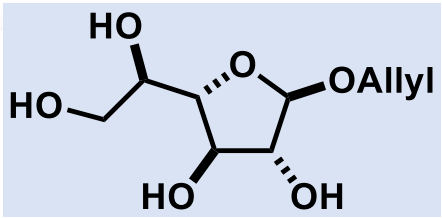

Altona-Sundaralingam pseudorotational phase angle: P

$$\tan P = \frac{(\phi_2 + \phi_4) - (\phi_1 + \phi_3)}{2\phi_0 (\sin 36^\circ + \sin 72^\circ)}$$

where φ_0-φ_4 are endocyclic torsion angles

φ_m describes the extent of puckering of the ring or the displacement from planarity

$$\phi_m = \frac{\phi_0}{\cos P}$$

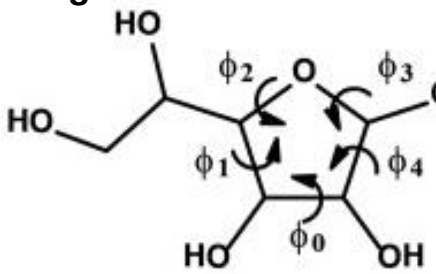

ϕ_0 = C1–C2–C3–C4
ϕ_1 = C2–C3–C4–O4
ϕ_2 = C3–C4–O4–C1
ϕ_3 = C4–O4–C1–C2
ϕ_4 = O4–C1–C2–C3

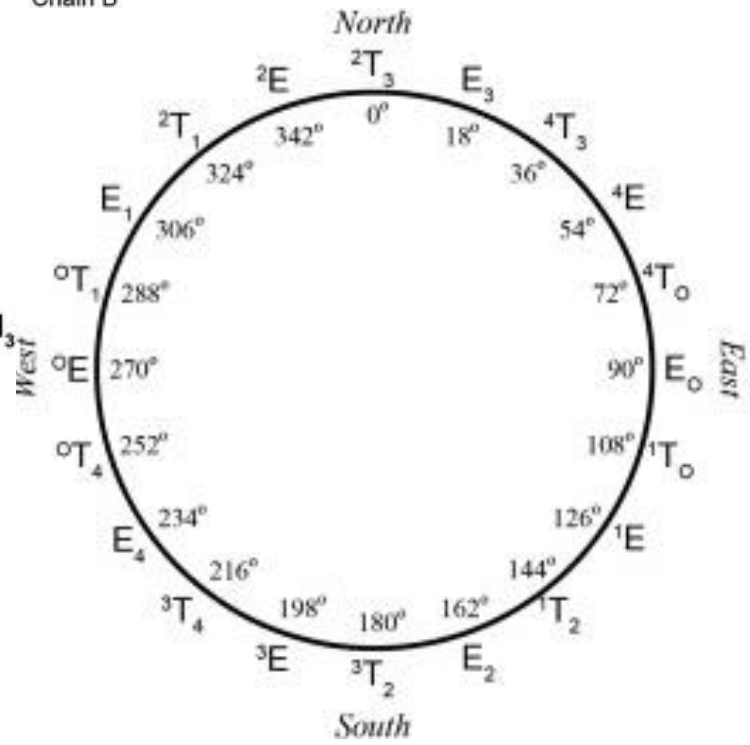

calculation data from X-ray crystallography

Chain A: P = 105° → ^1T_O

Chain B: P = 57° → ^4E

Furanose ring shape can be precisely described by Altona-Sundaralingam pseudorotational phase angle

Altona, C.; Sundaralingam, M. *J. Am. Chem. Soc.* **1972**, *94*, 8205.
Richards, M. R.; Bai, Y.; Lowary, T. L. *Carbohydr. Res.* **2013**, *374*, 103.

Ring Conformational Analysis of the Binding α-KO

Cremer-Pople parameters : θ, φ, Q
Q: puckering amplitude (deviation from the perfectly flat six-membered ring at Q = 0)

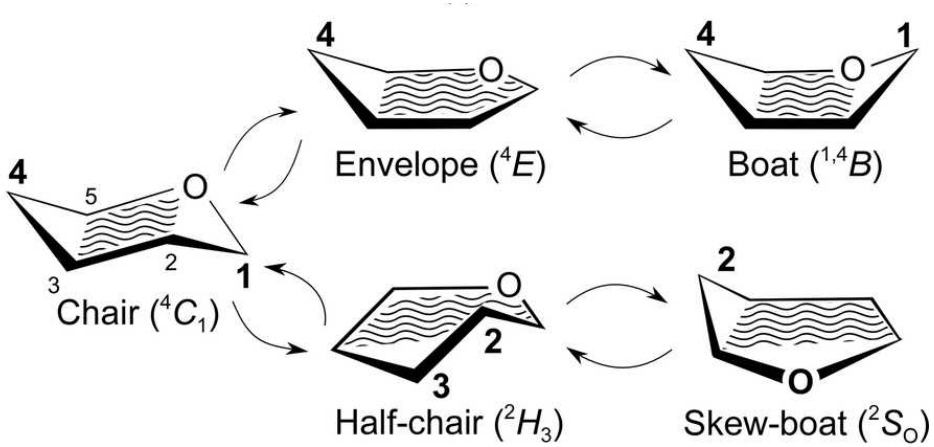

conformation of allyl-α-KO
calculation data from X-ray crystallography
θ = 9.5°, φ = 264.6°, *Q* = 0.58 Å → $^4C_1$

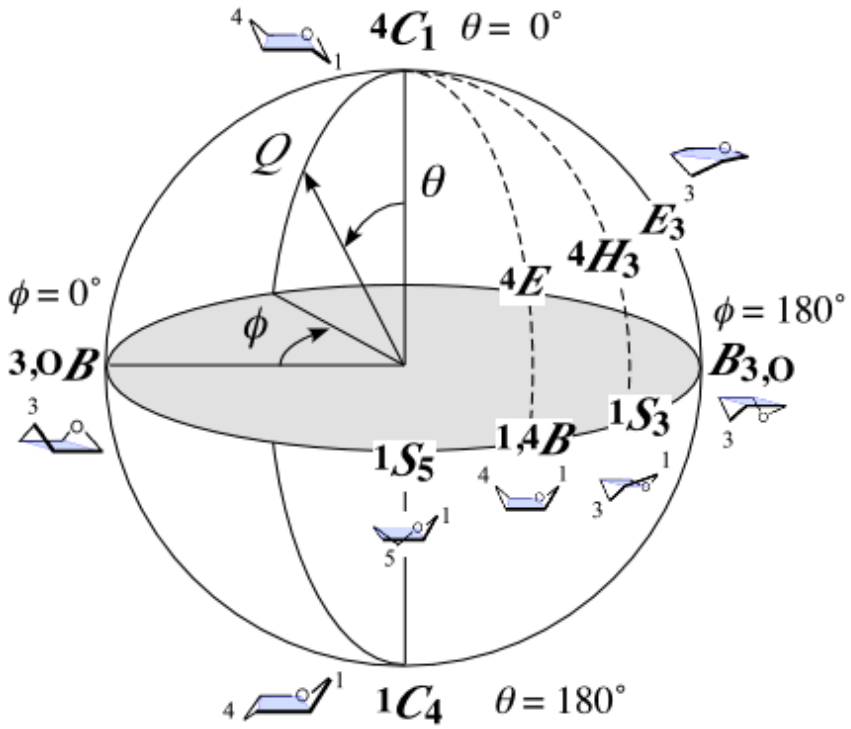

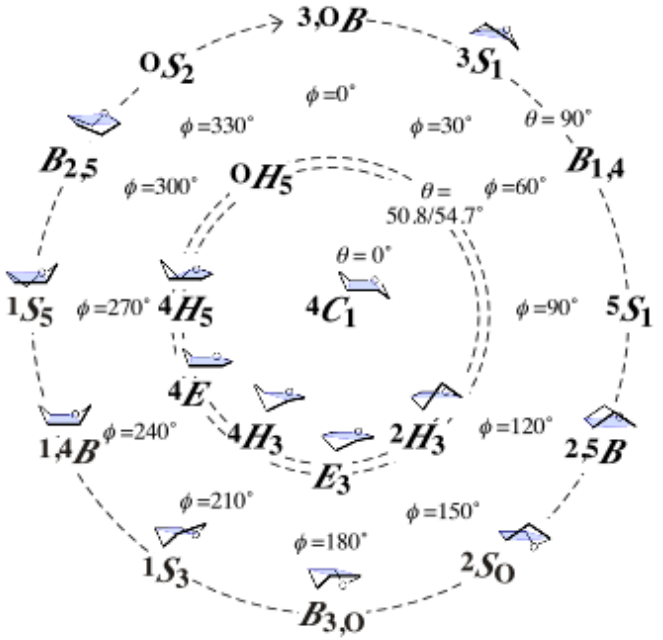

Pyranose ring shape can be precisely described by Cremer-Pople parameters

Cremer, D.; Pople, J. A. *J. Am. Chem. Soc.* **1975**, *97*, 1354.

Biolayer Interferometry (BLI) Competition Assay

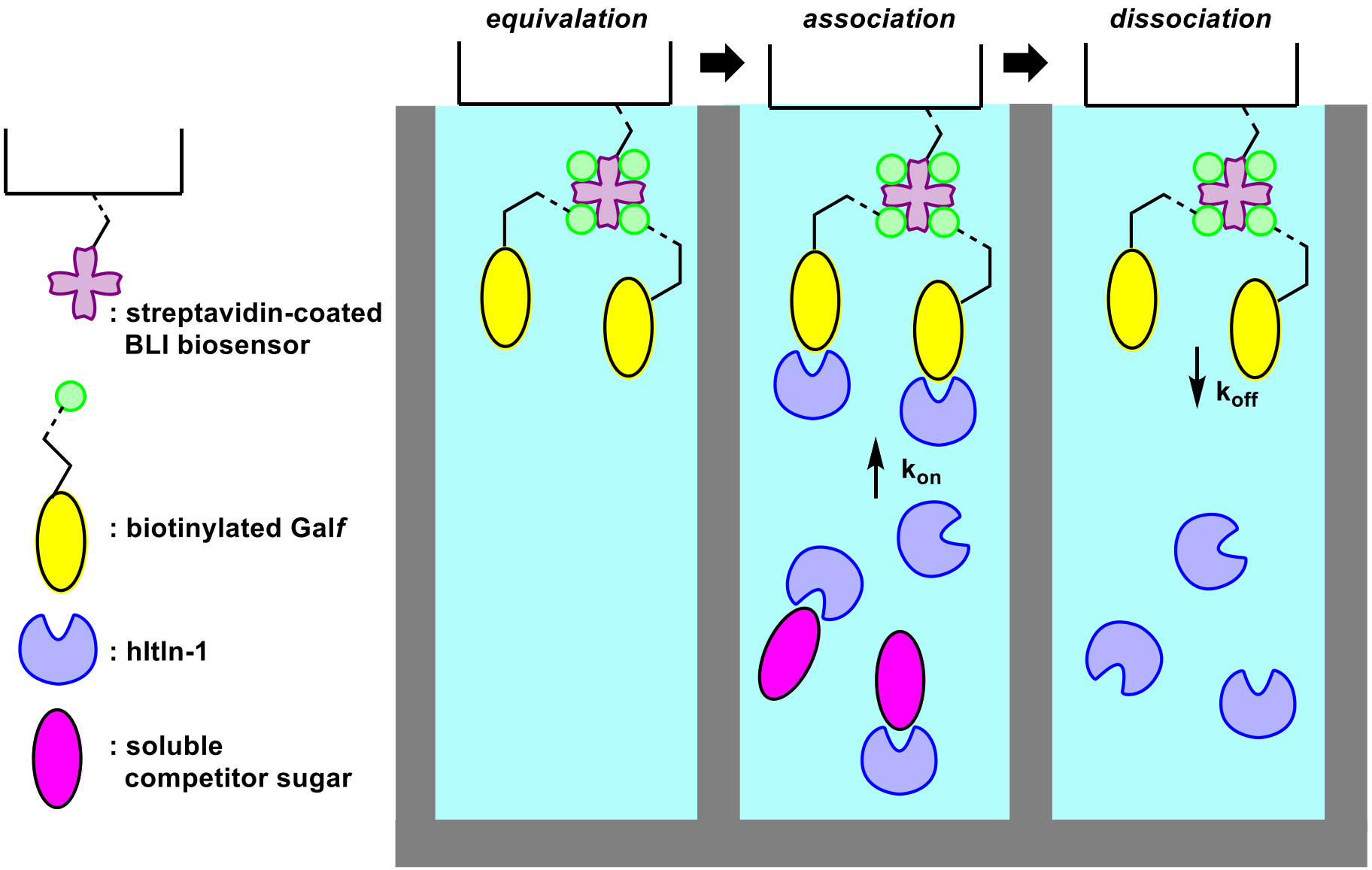

Biotinylated galactofuranose (Gal*f*) was immobilized on streptavidin-coated biosensors and incubated with hItln-1 in the presence of varying concentrations of soluble monosaccharides

Parameters Found by Biolayer Interferometry

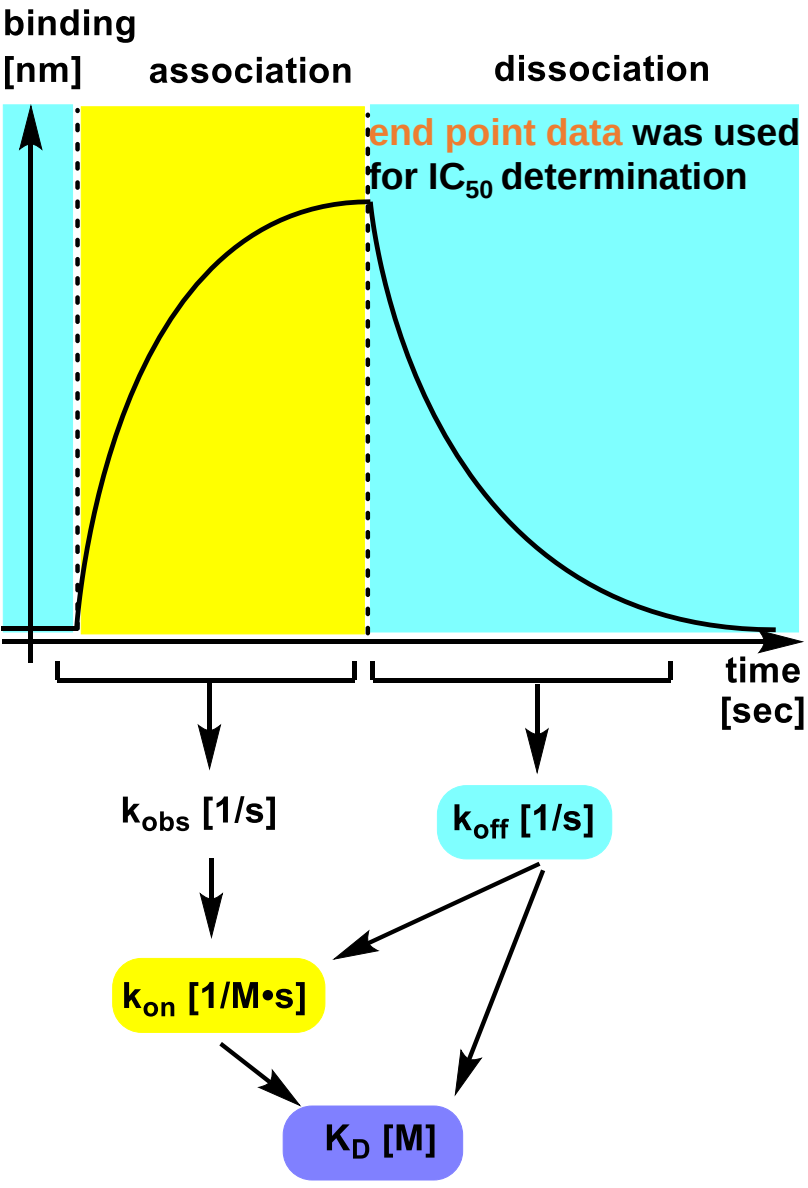

BLI of monosaccharides in competition with immobilized Gal*f*

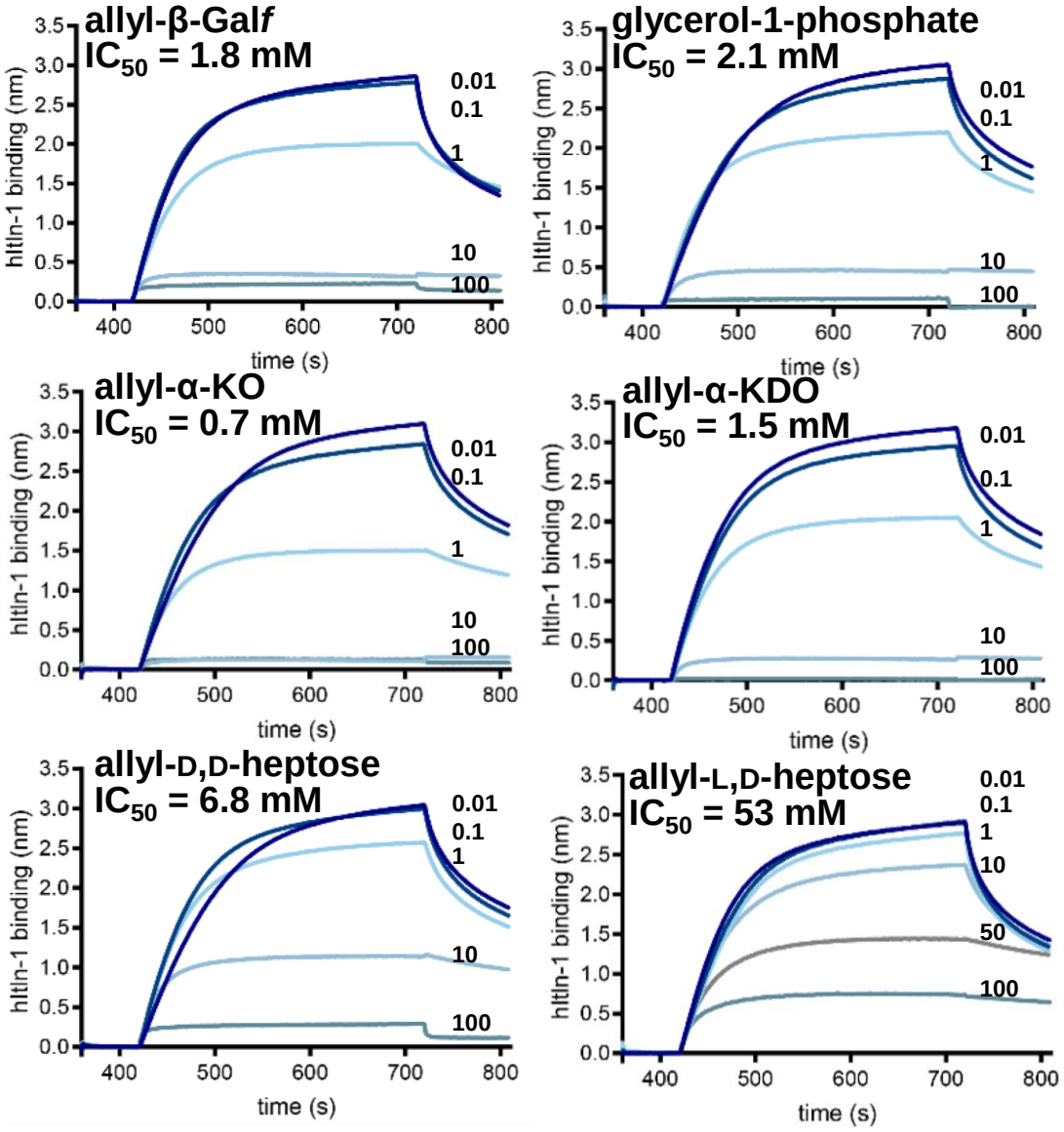

BLI can reveal kinetic constants ($k_{on,off}$), dissociation constants (K_D), and inhibitory concentrations (IC_{50})

Multivalency in Lectin-Glycan Recognition

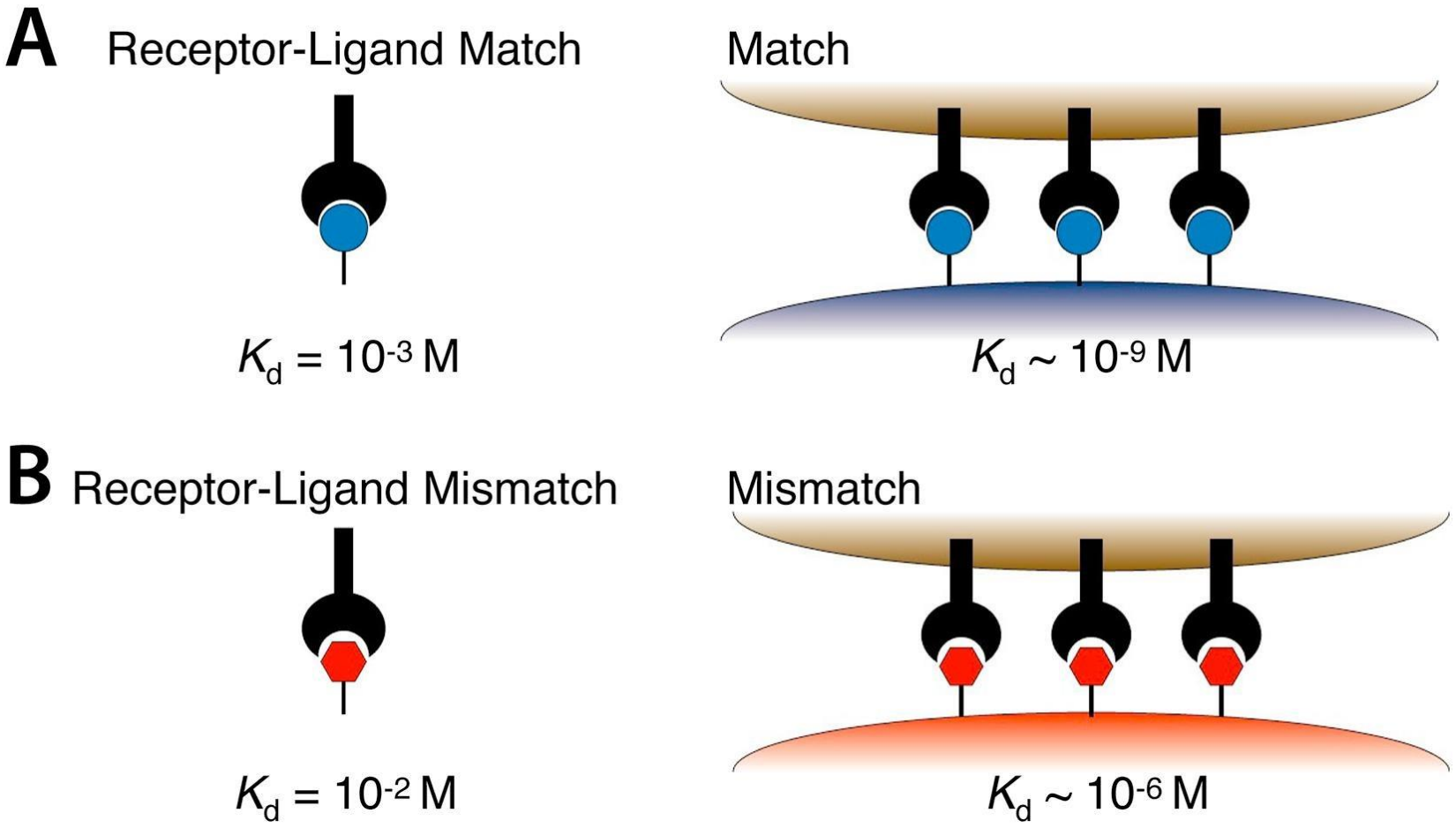

The discrimination between D,D-heptose and β-Galf arises from multivalent interactions, whereby small differences in binding are amplified